Southeastern Geology: Volume 38, No. 4
August 1999

Editor in Chief: S. Duncan Heron, Jr.

Abstract

Academic journal published quarterly by the Department of Geology, Duke University.

SOUTHEASTERN GEOLOGY

PUBLISHED

at

DUKE UNIVERSITY

Editor in Chief:

Duncan Heron

This journal publishes the results of original research on all phases of geology, geophysics, geochemistry and environmental geology as related to the Southeast. Send manuscripts to **DUNCAN HERON, DUKE UNIVERSITY, BOX 90233, DURHAM, NORTH CAROLINA 27708-0233**. Phone: 919-684-5321, Fax: 919-684-5833, Email: heron@eos.duke.edu Please observe the following:

1) Type the manuscript with double space lines and submit in duplicate.
2) Cite references and prepare bibliographic lists in accordance with the method found within the pages of this journal.
3) Submit line drawings and complex tables reduced to final publication size (no bigger than 8 x 5 3/8 inches).
4) Make certain that all photographs are sharp, clear, and of good contrast.
5) Stratigraphic terminology should abide by the North American Stratigraphic Code (American Association Petroleum Geologists Bulletin, v. 67, p. 841-875).

Subscriptions to *Southeastern Geology* for volume 38 are: individuals - $18.00 (paid by personal check); corporations and libraries - $24.00; foreign $28. Inquires should be sent to: **SOUTHEASTERN GEOLOGY, DUKE UNIVERSITY, BOX 90233, DURHAM, NORTH CAROLINA 27708-0233**. Make checks payable to: *Southeastern Geology.*

Information about SOUTHEASTERN GEOLOGY is on the World Wide Web including a searchable author-title index 1958-1996. The URL for the Web site is:

http://www.geo.duke.edu/seglgy.htm

SOUTHEASTERN GEOLOGY is a peer review journal.

ISSN 0038-3678

SOUTHEASTERN GEOLOGY

Table of Contents

Volume 38, No. 4

August 1999

SOUTHEASTERN GEOLOGY
V. 38, No. 4, August 1999, p. 239-257

A NEOPROTEROZOIC PALEOSURFACE AND ASSOCIATED COLLUVIAL AND FLUVIAL DEPOSITS, SHENANDOAH NATIONAL PARK, VIRGINIA

DILLIARD, K. A.

Department of Geology
Northern Arizona University
Box 4099
Flagstaff, AZ 86011-4099

SIMPSON, E. L.

Department of Physical Sciences
Kutztown University
Kutztown, PA 19530

NOTO, R. C.

Department of Geological Sciences
University of Nevada — Las Vegas
Las Vegas, NV 89154

ABSTRACT

Near Big Meadows in Shenandoah National Park, Virginia, the Mesoproterozoic Saddleback Mountain Charnockite Suite (SMCS) is exposed in an inlier through the Neoproterozoic Catoctin Formation. An investigation of the inlier contact, a nonconformity, and the interrelationship of the sediments and volcanic units of the Catoctin Formation provides a unique opportunity to: 1) reconstruct characteristics of the topography preserved below the nonconformity, 2) describe and interpret clastic facies associated with a preserved paleotopographic high, and 3) interpret the processes related to the interaction of topography, sedimentation and volcanism in this Neoproterozoic rift setting.

In this study area, the SMCS lies beneath the nonconformity surface and is covered with colluvium. The preserved SMCS erosional surface represents one flank of a more extensive paleohigh. As exposed in the inlier, the minimum local topographic relief was 220 meters and the average slope was approximately 20% or 11 degrees.

Within the Catoctin Formation, adjacent to the nonconformity, three facies were recognized: 1) breccia facies, 2) sorted sandstone and conglomerate facies, and 3) soft-sediment deformed heterolithic facies. The breccia facies is poorly sorted and apparently structureless. Clasts within the breccia beds are mainly basement, SMCS, with a very minor basaltic clast component. The breccia facies is interpreted to represent colluvial deposition in which detritus was generated from grusification of the exposed SMCS. The sorted sandstone and conglomerate facies consists of massive sandstone and conglomerate beds that grade into overlying sandstone units. The sorted nature of this facies indicates fluvial transport and reworking of the colluvial material. The soft-sediment deformed heterolithic facies varies from predominately sandstone to mudstone; all slabs display soft-sediment deformation features. This facies most likely reflects deposition in possibly a lacustrine or floodplain setting. Lacustrine environments developed as a consequence of lava flows damming the valleys fluvial drainage. Soft-sediment deformation could have resulted from several different or a combination of the following mechanisms: dewatering, debris flow movement, earthquakes or the interaction of lava and water-saturated sediments.

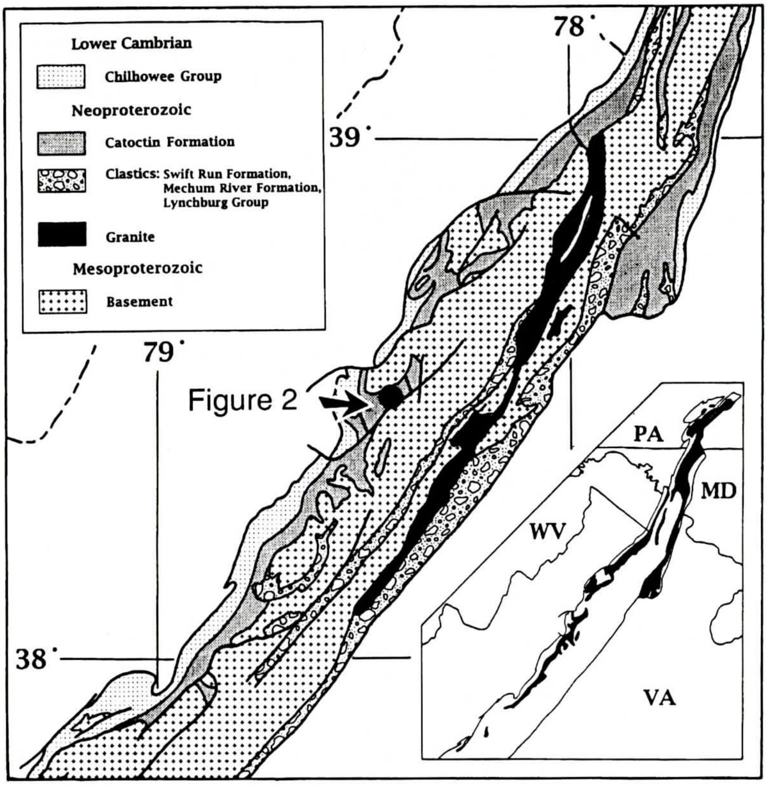

Figure 1. Geologic map of the Blue Ridge in central Virginia (modified from Rankin, 1993). Inset map shows distribution of Catoctin Formation throughout the Blue Ridge.

INTRODUCTION

Two distinct phases of rifting, ~720 and ~580 Ma, with associated sediments and volcanism, are recognized within the southern Appalachians (Badger and Sinha, 1988; Aleinikoff and others, 1995; Tollo and Aleinikoff, 1996) and are attributable to the fragmentation of Rodina (Unrug, 1997) and the subsequent development of the Laurentian passive margin (Wehr and Glover, 1985; Simpson and Eriksson, 1989; Aleinikoff and others 1995). During the last phase of extension, the Neoproterozoic Swift Run and Catoctin formations accumulated within an evolving rift basin.

The Swift Run Formation and overlying Catoctin Formation crops out on the flanks of the Blue Ridge Province in central and northern Virginia (Figure 1; Wehr and Glover 1985; Badger, 1986, 1992; Badger and Sinha 1988). The older Swift Run Formation is primarily composed of sediments with minor volcanic beds. Mafic volcanic rocks and subordinate volumes of clastic rocks characterize the younger Catoctin Formation.

Within the study area, both formations infill and preserve paleotopography developed on Mesoproterozoic basement. Preserved Neoproterozoic topography is well exposed in the Rose River inlier within Shenandoah National Park (Figure 2). The inlier was first mapped by Reed (1955) and its outcrop pattern was latter refined by Gathright (1976). The basement units, Saddleback Mountain Charnockite Suite (SMCS), were subsequently defined by Batholomew and Lewis (1984) and Hughes and others (1997). The inlier and the nonconformity surface are exposed along the Hogbranch and Rose River drainages. Additionally, trails and a fire road heading south from Fishers Gap cross the nonconformity contact between the and the Catoctin Formation (Figure 2). In Shenandoah

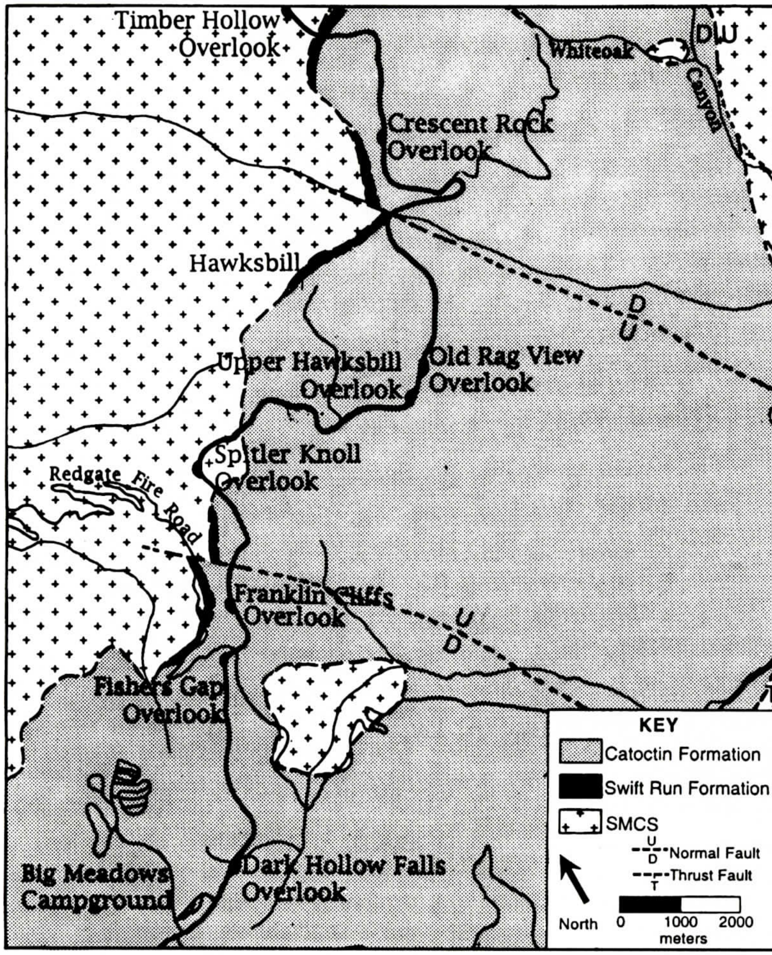

Figure 2. Geologic map of the Big Meadows Campground area (modified from Gathright, 1976). The Rose River Inlier is located northeast of Big Meadows Campground in Shenandoah National Park, VA within the Big Meadows 7 1/2 minute quadrangle.

National Park, additional inliers expose the paleotopography associated with the contact, but have more limited access. Reed (1955; 1969) and Gathright (1976) recognized that these inliers expose the buried relief on the basement and concerning the relative influence it exerted on local sediment supply during subsequent Neoproterozoic deposition.

This paper documents the paleotopography on the basement and associated sediments in Rose River inlier (Figure 2). Specifically we: 1) reconstruct the local relief and slope developed on the topography; 2) describe sedimentary facies adjacent to a basement high; 3) interpret the depositional environment in which the facies accumulated; 4) examine nonconformity surface in hand specimen; 5) demonstrate that the land surface developed on the Mesoproterozoic SMCS was not characterized by extensive soil development but was grusified and covered with colluvium; and 5) examine the interaction of topography, colluvial sedimentation and volcanism.

STRATIGRAPHY

Within the study area, three stratigraphic units are recognized from oldest to youngest, the SMCS (basement), nonconformably overlain by the Swift Run and Catoctin formations

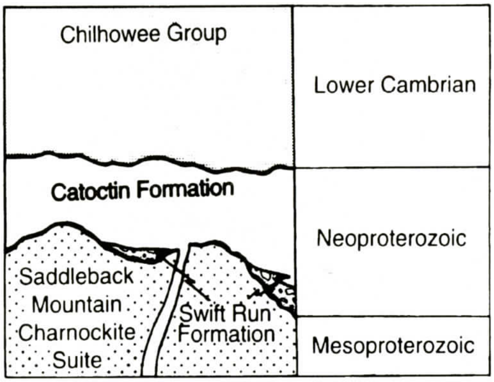

Figure 3. Stratigraphy in the Big Meadows study area.

(Figure 3).

The Mesoproterozoic age SMCS is highly variable in composition but primarily consists of weakly foliated charnockitic to quartz mangeritic lithologies (Reed 1955; 1969; Gathright, 1976), similar to the Pedlar River Charnockite Suite described by Hughes and others (1997) found further south, approximately 80 km from the study area. Locally, hydrothermal alteration, possibly during Neoproterozoic volcanism (Tollo and Hudson, 1996) or more likely by Paleozoic metamorphism, has converted a percentage of the charnockites to unakite, characterized by epidote, pink feldspar and blue quartz (Reed 1955; 1969; Gathright, 1976).

The Neoproterozoic Swift Run Formation is highly variable in thickness and consists of feldspathic sandstones, matrix-rich conglomerates, and minor amounts of felsic tuffs, basalt flows, laminated mudstones, and siltstones. The Swift Run Formation is typically more intensely deformed than similar lithologies within the overlying Catoctin Formation. In the study area, the Swift Run Formation is exposed as a series of mappable, isolated channel forms that have widths of 2400 and 4000 meters (Gathright, 1976). A Swift Run Formation channel-fill exposed along Red Gate Fire Road (Figure 2), was measured to be up to 48 meters thick.

The Catoctin Formation is composed of mafic volcanic rocks with lesser amounts of feldspathic and lithic sandstones and conglomerates. Mafic flows within the Catoctin Formation in the Big Meadows area contain volcanic features, such as, massive aphanitic basalt, colum-

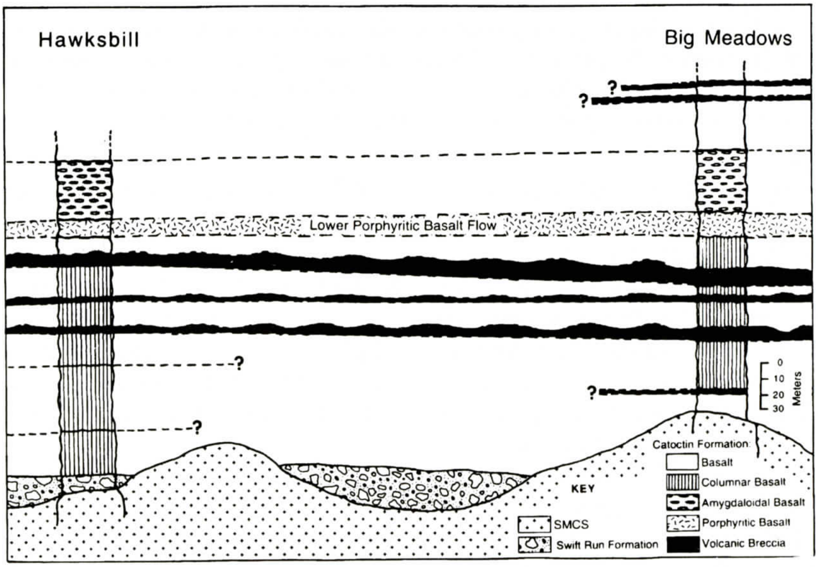

Figure 4. Panel diagram showing correlation of basalt flows and measured sections from Big Meadows Campground and Hawksbill Mountain (modified from Badger, 1992). Sections were reexamined by authors and base of panel reflects the geometry of the Swift Run Formation as determined during the course of this study. Distance between the Hawksbill and Big Meadows section is approximately five kilometers (Badger, 1992).

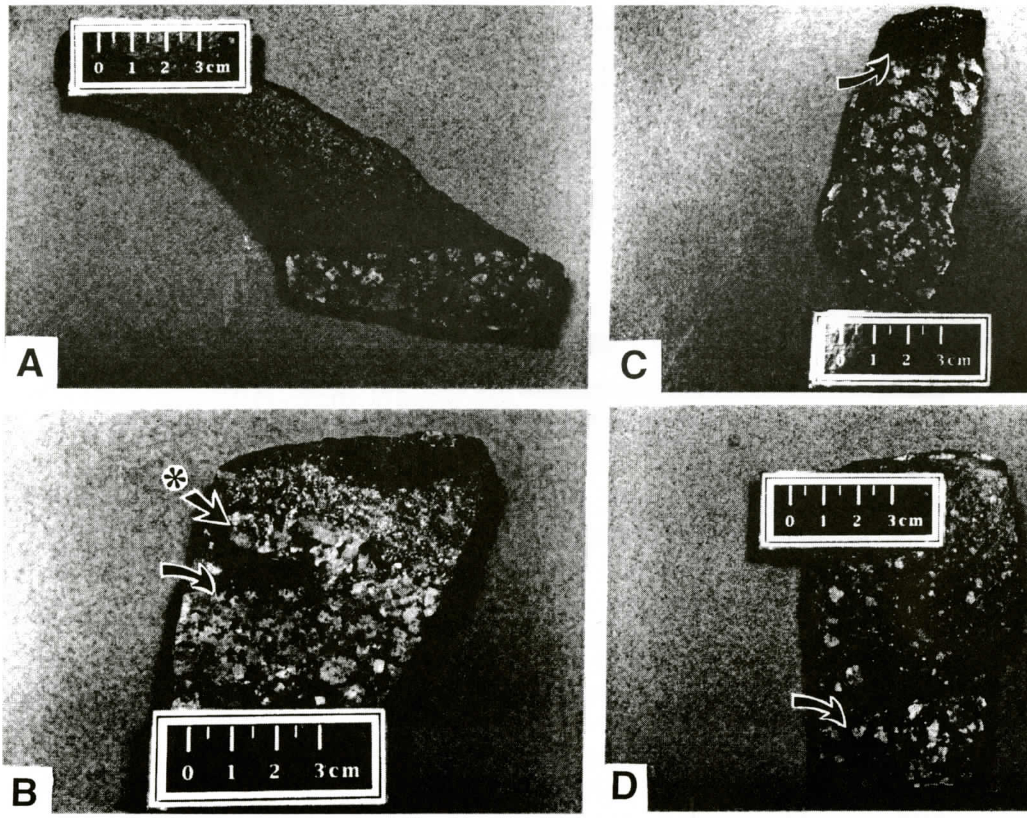

Figure 5. Photographs of slabs that contain the nonconformity. Arrows point to the nonconformity surface. A) Structureless medium-grained sandstone in sharp contact with the SMCS. Note the sharp contact exhibits slight relief. B) Tabular clast of SMCS above the nonconformity show by arrow with asterisk. Grain size of sandstone enclosing clasts varies from fine to coarse. C) Fine to medium-grained sandstone overlying the SMCS. Note the relief on the contact. D) Poorly sorted breccia above the SMCS.

nar joints, amygdules, flow breccias, preserved porphyritic textures, and rare pillow lava (Figure 4; Reed, 1955; Reed and Morgan, 1971; Gathright, 1976; Badger, 1986; 1992). Flow breccias form a series of laterally continuous resistant benches that are traceable on airphotographs and in the field. Two porphyritic basalt flows, with phenocrysts of albitized feldspars, serve as mappable marker flows to subdivide the stratigraphy (Reed 1955; 1969; Figure 4). The top of the lowermost porphyritic flow of Reed (1955) and Reed and Morgan (1971) is located at a maximum of 165 meters from the base of the oldest delineated basalt of the Catoctin Formation and onlaps the paleotopography (Figure 4). At Big Meadows and Hawksbill Mountain, Badger (1986; 1992) recognized 10 and 9 distinct mafic flows, respectively (Figure 4). Upon correlating these flows, Badger (1992) delineated 11 distinct flows with a combined thickness of 205 meters, between Hawksbill Mountain and Big Meadows with some flows not present at both localities. Conglomerates and sandstones rest directly on SMCS with thin sheets of clastics separating mafic lava flows.

AGE CONSTRAINTS

Radiometric ages were gleaned from mafic and felsic volcanic rocks of the Catoctin Formation. North of the study area, metarhyolites, restricted to the lowermost Catoctin Formation, yield a zircon U/Pb age of 564 ± 9Ma (Alleinikoff and others, 1995). Additionally, Alleini-

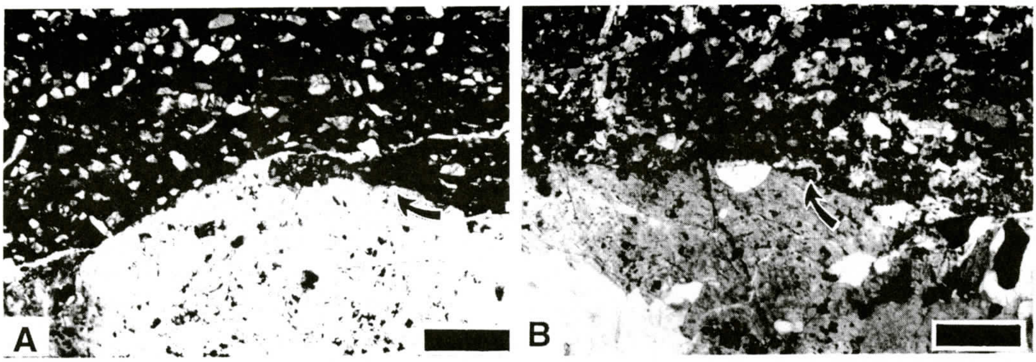

Figure 6. Photographs of thin sections, in plain polarized light, that contain the nonconformity surface. A) Shows the irregular surface of the nonconformity overlain by a sandstone. B) Contact surface with visible fracturing of grains within the basement. Scale is 1 millimeter.

koff and others(1995) report an age of 572 ± 5 Ma for an interpreted feeder dike to Catoctin Formation basalts. Rb-Sr whole-rock age dating methods applied to mafic volcanic rocks south of the study area indicate an age of 570 ± 36 Ma (Badger and Sinha, 1988). These radiometric age constraints place the Catoctin Formation within the Neoproterozoic Cryogenian or Vendian periods; the Varanger/Marinoan Glaciations, ~570-590 Ma, occur during this time interval (Narbonne, 1998).

METHODS

The nonconformity between the SMCS and Catoctin Formation was reexamined in detail, employing float mapping techniques (Figure 2). Old prospecting pits, excavated in search of copper mineralization, served as aids to delineate the nonconformity contact within a few meters or less. Outcrops are limited and are exposed on scraped roads, drainages and the prospecting pits. Blocks and hand samples of the nonconformity were found along the contact and used to describe the nature of the contact.

Petrology and sedimentary structures were determined from the 60 specimens that were slabbed and thin sectioned as part of this study. Field observations were integrated with those gleaned from polished rock slabs and thin sections allowing samples to be grouped into sedimentary facies and processes to be interpreted.

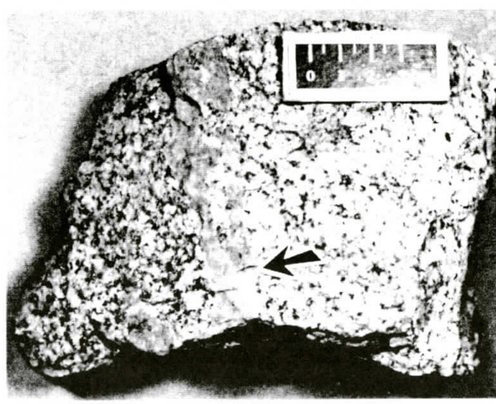

Figure 7. Photograph of slab with sediment-filled crack in the SMCS. Arrow points to crack fill. Note the geometrical match across the crack.

NONCONFORMITY SURFACE

Description

The Rose River inlier exposes approximately 0.2 km^2 of the SMCS (Figure 2). Specimens preserving the nonconformity were often found in tailings associated with prospecting pits (Figure 5A-D). In slab sections, the nonconformity displays small-scale relief of 0.5 cm over 7 cm of lateral length (Figure 5A and 6A-B). In hand specimens, no substantial visible evidence of weathering or alteration of feldspars was evident in the SMCS below the contact. However, in several thin sections, feldspars and quartz grains are fractured below the contact.

In the field, fractures were observed parallel to the nonconformity surface. Within slabs, fractures are filled with sand- to silt-size sediment and range in width from 0.1 to 0.4 cm and length from 6.0 to 10.0 cm (extent of slab) (Figure 7). Sidewall geometry and the match of grain type and shape across the fracture permit distinction of fracture fill from the void fills found within the colluvium, described later. Small pebble-size basement clasts are present within some fracture fills (Figure 7). Fracture orientation could not be determined in the field. Reed (1955) and Gathright (1976) report fractures with associated red alteration that penetrate at least 15 meters into the underlying SMCS north of the study area.

Interpretation

Several factors, such as, tectonism, drainage density and structure, unequal erosion and bedrock character, reinforcement mechanisms, moisture, and subsurface weathering resulting in lowering of the landsurface, promote preservation of paleolandforms (Twidale, 1976; 1997). Numerous fossil landscapes were recognized throughout the world at differing geographic scales and from disparate geologic times (*e.g.* Twidale, 1976; 1997; Fairbridge and Finkl, 1980; Wielemaker and van Dijk, 1981; Taylor and others, 1985; Ollier and others, 1988; deVillers, 1989; Smith and Bishop, 1993; Battiau-Queney, 1996).

Eruption of copious amounts of lavas can potentially preserve a pre-eruptive landscape (Battiau-Queney, 1996). Examination of Tertiary-age volcanic rocks in New South Wales, Australia showed that basalt flows buried and preserved the pre-eruption drainage pattern (Taylor and others, 1985; Smith and Bishop, 1993). The preserved sub-basaltic topographic relief exceeds 200 m and the paleosurface is characterized by fresh to highly weathered bedrock (Taylor and others, 1985).

In contrast, the nonconformity surface exposed the Rose River Inlier appears not to display extensive pedogenesis or soil profiles (Figure 5A-D and 6A-B). Weathering is restricted to grusification, coarse fragments resulting from granular disintegration of crystalline rocks. Fracture fills are the most readily identifiable exposure-related feature preserved in the basement (Figure 5B and 7). Fractures associated with the degradation of igneous rocks form by numerous mechanisms at different burial depths (Whalley and others, 1982) and accelerate the weathering of these rocks. Detritus generated during grusification were washed into these open fractures within the basement (Figure 7).

Calculation of median gradient

The average strike and dip, 070 and 12 degrees to the southeast respectively, as determined from various basalt flows, was calculated from measurements reported on geologic maps of Reed (1969) and Gathright (1976) in the vicinity of the Rose River Inlier. Using this average strike, the furthest point in the up dip direction of the contact and tangent to the inlier was selected as a point of rotation (Figure 8). Elevations of the contact were rotated about the strike line in order to correct for the average tectonic dip; points further from the strike line were adjusted in elevation a greater amount than those in proximity (Figure 8). Following this process, two outcrop elevations of the lower porphyritic flow, lowest most onlapping the paleohigh, was used to test if the rotated flow elevations were reasonable; the porphyritic flow unit rotated to a nearly horizontal, with the same corrected elevation on both sides of the inlier. The recalculated elevations of the nonconformity surface were contoured (Figure 8). The paleoslope was calculated perpendicular to the corrected surface contours. The maximum slope obtained within the Rose River Inlier was determined to be approximately 20% grade or 11 degrees. This processes does not take into account plunging folds or other structural complications, but gives an approximation.

The overall geometry of the material removed by modern erosion, breaching of the Catoctin Formation to form the inlier, could not be considered. For example, the paleosurface may have been more geometrically diverse concave or convex shapes as opposed to the a relatively

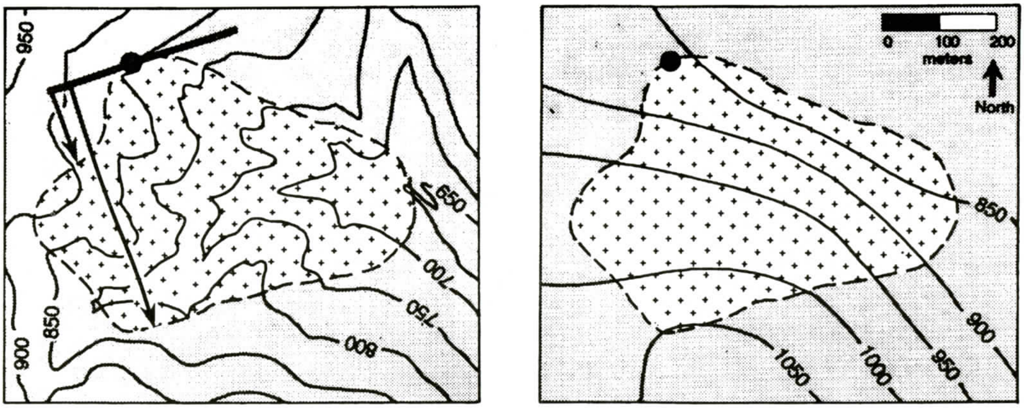

Figure 8. Rose River Inlier. Shaded pattern is Catoctin Formation. Cross pattern is SMCS. A) Original elevations in meters. Strike line is 070 and dip is 12 degree to the southeast. The contact closer to the strike line had lesser elevation correction then the contact further from the rotation line. Float mapping technique had to be employed, the contact is accurate to within a few meters or less. B) Resorted elevations after the tectonic dip has been removed.

flat uniform surface employed in our contour methods.

Calculation of minimum relief

The paleotopographic relief can be estimated by adding the maximum thickness of the Swift Run Formation to the thickness of lower part of the Catoctin Formation that onlaps the inlier. The maximum thickness of 48 meters, was measured along a channel-form exposed on Red Gate Road. This thickness of the Swift Run Formation was determined from the base of the valley fill to the base of the first basalt flow of the Catoctin Formation. This measurement does not consider compaction or volume loss by metamorphism. The position of Reed's (1955; 1969) lowermost porphyritic flow was extrapolated into the nonconformity surface contact. The lowermost porphyritic flow truncates against the inlier (Reed 1956; 1969). Therefore, the 165 meters of basalt, as measured by Badger (1992), that is below the lower porphyritic horizon must be added to Swift Run Formation thickness. An additional thickness of 25 meters occurs from above the lower porphyritic flow to the top of the inlier, thus increasing the local relief to ~230 meters. The preserved paleotopography may have been accentuated by then-active tectonics or diminished by erosion before buried by subsequent lava flows.

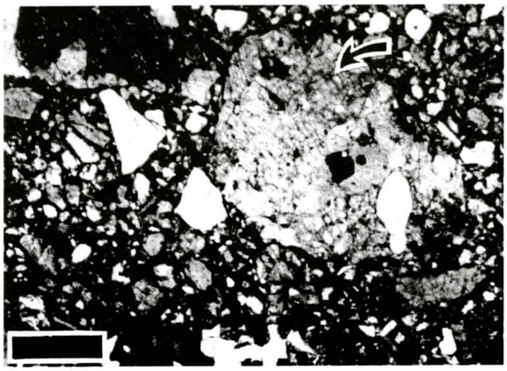

Figure 9. Photograph of thin section, in plain polarized light, showing a granitic clast within medium sand. Scale is 1 millimeter. Note the angularity of the grains.

FACIES OF THE CATOCTIN FORMATION

Data from thin-section point counts indicate sandstones are feldspathic to lithic in composition. The most common lithic grain type is basement (SCMS) with lesser amounts of mafic volcanic fragments (Figure 9). Not all samples contain mafic volcanic fragments but all contain plutonic clasts of varying percentages. Most specimens display extensive metamorphic replacement of minerals by the addition of epidote and chlorite, often as euhedral crystals

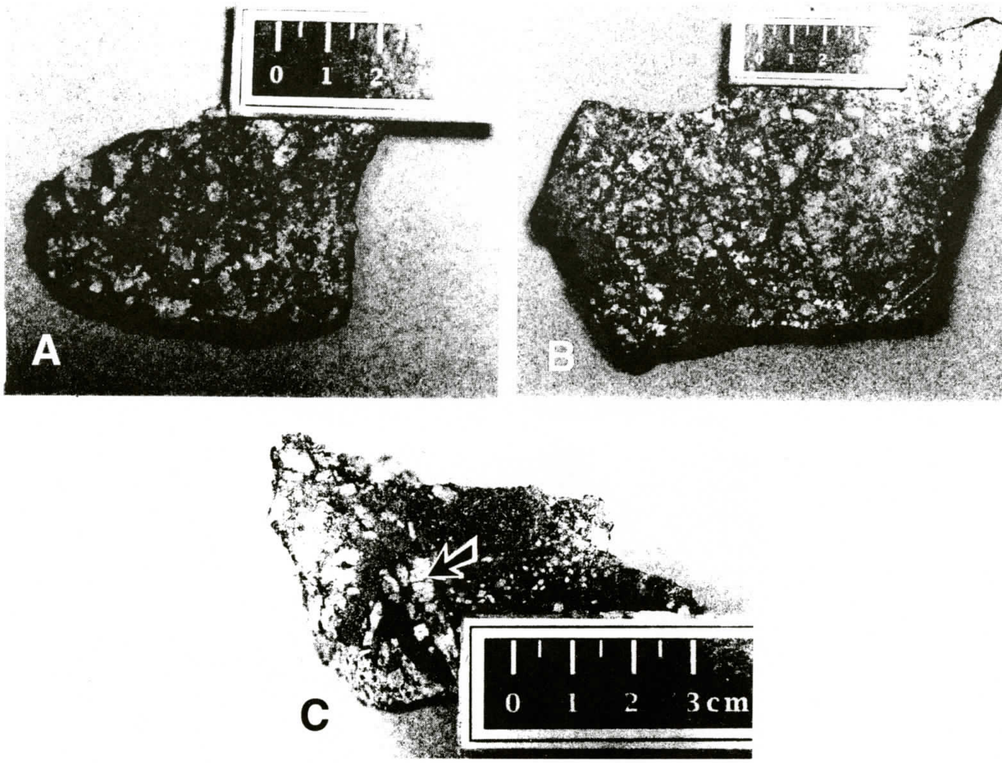

Figure 10. Photographs of the breccia facies slabs. A) Poorly sorted breccia. B) Poorly sorted breccia. Note dark basalt clasts. C) Tabular-shaped clasts of basement in a sand-dominated matrix.

cross-cutting primary sedimentary fabrics.

Based on the petrology and preserved sedimentary structures, three facies are identified, described and interpreted. From most to least common, the facies are: 1) breccia facies, 2) sorted sandstones and conglomerates facies, and 3) soft-sediment deformed heterolithic facies.

Breccia Facies

Description

The breccia facies is poorly sorted with the largest clast in the pebble-size range (Figure 5D, 10A-C). Basement clasts, the most common type within the breccia facies, are mostly angular, although they range from vary rounded to sub-rounded. Sometimes, basement clasts exhibit a tabular morphology (Figure 5B and 10C). When present in this facies, basalt clasts are always angular (Figure 10B). Poorly sorted, silt-size grains represent the finest fraction found in the matrix.

In one slab, clast size decreases vertically from 8 cm to 4 cm, but most often grading is absent, and clast-size distribution and sorting is consistent from sample to sample. Deposits are otherwise massive (featureless); no other sedimentary structures are apparent (Figure 5D and 10A-C).

Within slabs of breccia, voids between clasts are filled with finer-grained sediment (Figure 11A-C). Void fills range from a width of 0.1 to 0.6 cm and a length from 4.0 to 10.0 cm (extent of slab). Void fill between clasts varies from simple to complex (Figure 12). Simple void fills include graded beds from medium- to fine-grained sandstone, medium-grained sandstone to siltstone or graded siltstone (Figure 11B and 11C). Sandstones are lithic in composition. One simple fill grades from coarse-grained sandstone with small pebbles into an overlying silt-

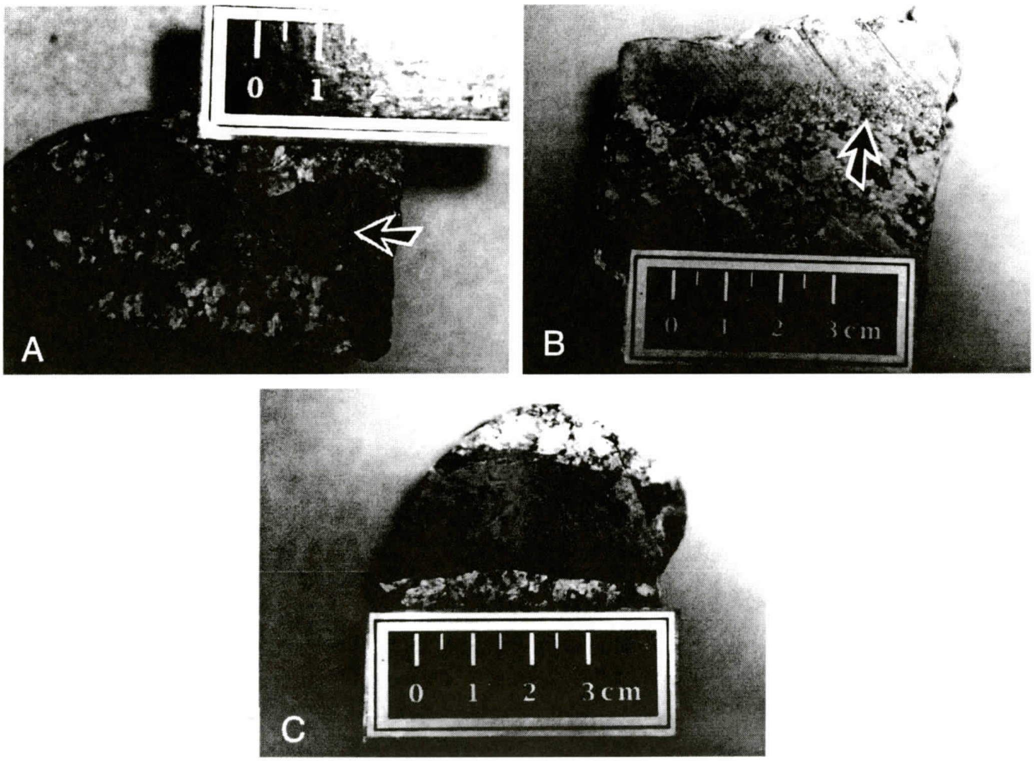

Figure 11. Photographs of preserved void fills. A) Complex crack fill. Note the variation in sand size across the crack fill in the slab. B) Simple graded void fill. Fill grades upward from medium to coarse sand to siltstone. C) Siltstone filled crack.

stone. Complex void fills include fills with multiple graded layers consisting of medium- to fine-grained sandstone or medium-grained sandstone to siltstone (Figure 11A. In one fracture, walls are coated with siltstone which passes towards the center into coarse sand-size material. Multiple graded beds of medium- to fine-grained sandstone were identified filling one void.

The breccia facies is restricted to the Catoctin Formation adjacent to the inlier and similar lithologies were not identified separating basalt flows throughout the extent of the Catoctin Formation by any previous worker (Reed, 1955; 1969; Reed and Morgan, 1971; Gathright, 1976; Badger, 1986; 1992; Badger and Sinha, 1988).

Interpretation

The coarse-sand size of detritus and the absence of large basement blocks over 10 cm in diameter in this facies is attributable to the grusification of the exposed basement. Quartz boulders, over 40 cm in diameter, and basement clasts with an approximately 10 cm maximum diameter, have been reported by Bartholomew (1977) from the Swift Run Formation south of Shenandoah National Park. Mechanisms which generate grus are varied and include, salt weathering (Fahey, 1985), mineral hydration (Eggler and others, 1969; Isherwood and Street, 1976), crack propagation and associated weathering (Whalley and others, 1982), and buttressed expansion and associated accelerated weathering (Folk and Patton, 1982). Deflection of dikes traversing from granite into grus, allowed Folk and Patton (1982) to demonstrate that approximately 50% increase in the volume takes place in generating the grus. As a consequence, even exposed relatively low-relief granitic hills can make a significant contribution of detritus to the drainage basin.

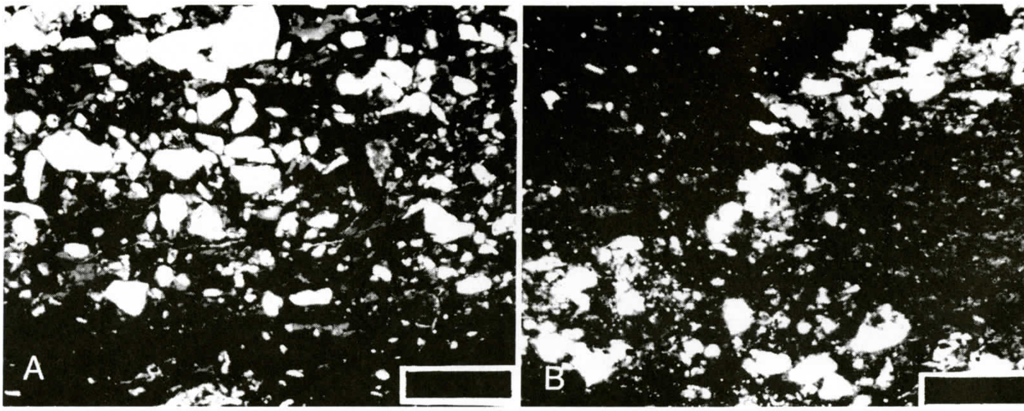

Figure 12. Photographs of thin sections, in plain polarized light, of sediment within a crack (the same crack). Note the different grain sizes ranging from sand to silt. May possibly indicate two distinct infill histories. Scale is 1 millimeter.

Tabular clasts in the deposits may have been caused by micro-sheeting joints paralleling the weathering granitic surface (Figure 5B and 10C). Folk and Patton (1982) argue that stresses generated along such fracture planes are significant when the rock is laterally buttressed or fixed. Even at small expansion rates, they argue, buttressing causes arching or tenting of the fractured sheet enhancing and accelerating the development of grus by water penetration and hydration of minerals. Soil seams separating joint blocks could mediate the stresses generated by this process (Folk and Patton, 1982).

The breccia facies is interpreted to reflect preserved colluvial deposits and associated secondary processes, such as sheet wash, that modified the colluvium. Variations in the sedimentary properties of these colluvial deposits, mainly grain size, may reflect differences in the topography of the depositional setting (Mills, 1987). This facies records two distinct depositional processes; first, the massive breccia composed solely of locally derived basement clasts records deposition as primary colluvium and second, the presence of complex void fills and basalt clasts indicates, at minimum, some reworking of the upper colluvial surface occurred.

Modern colluvial deposits move downslope at varying rates along a glide plane (Varnes, 1978; Bovis, 1986; Cronin, 1992) and in this case most likely the resistant granitic surface. In modern settings, movement of colluvial debris can be initiated by earthquakes (Keefer, 1984), precipitation or snowmelt events saturating sediments (Caine, 1980; Ellen and Fleming, 1987; Reneau and others, 1990) or by a variety of geomorphically slow processes (Gardner, 1983). Colluvial deposits are restricted proximally to a mountain front but may evolve into a debris flow during movement (Blair and McPherson, 1994a).

The presence of minor amounts of angular basalt clasts (Figure 10B) within a few specimens indicates that limited reworking of the colluvium by secondary process occurred possibly near the colluvial toe or on the upper surface of the depositional wedge. Basalt flows may have cropped out in an upslope or upvalley direction contributing detritus to the colluvium. Outcrops of basalt flows that were topographically higher, in contact with basement as opposed to colluvial deposits, can not be eliminated totally as a source, but no direct evidence supports their occurrence or eruptions from the granitic slopes. Within the basement inlier, cross cutting basaltic feeder dikes are not been reported. Eruption of basalts at a higher elevation would have a significantly lower preservation potential because instead of being subjected to burial by subsequent flows and detritus, they would have been subjected to weathering and erosional processes. The exact source of the basalt clasts is problematic.

Blair and McPherson (1994a) argue that colluvial sedimentation events, generated during extreme storm events, are often masked by latter modifications caused by lesser storm events. These lower magnitude storms transport sands, most often as sheet wash. Reworking of the upper colluvial surface, associated with lesser magnitude storm events, is indicated by the simple and complex void fills between clasts and some grain size segregation in slabs (Figure 11A-C). The voids, primary pore spaces, were most likely open after primary deposition of colluvium (breccia) and subsequently infiltration with sediment transported across the colluvial surface as indicated by the preservation of graded layers. Multiple graded beds may reflect sedimentation from pulses of single storms or multiple storm events. Significant transport of sediment and modification by sheet wash processes along the upper sediment surface of the colluvium is more likely to occur on the lower reaches of the colluvial slope because the runoff contribution is increased from higher elevations.

Studies of the interactions of lava flows and fluvial drainage also support lower reworking of the colluvium and mixing of basalt clasts. Inbar and others, (1995) and Smith (1988) demonstrated that lava flows will displace drainage to the periphery of a flow. In the Catoctin Formation depositional setting lateral displacement could have moved the drainage towards the valley edge as lava flows filled the valley increase the potential reworking.

Sorted Sandstones and Conglomerates Facies

Description

The sorted sandstone and conglomerate facies consists of fine- to coarse-grained sandstones with subordinate conglomerates (Figure 5A, 5C and 13A-C). The sandstones are massive, and are moderate to well sorted (Figure 5A, 5C, and 13A). Rare, basalt and basement clasts are present within the sandstone. Sandstone grains are subrounded to rounded. In one slab, massive, medium-grained sandstone is interbedded with a layer of conglomerate. The conglomerate is composed mostly of well rounded basalt clasts with basement clasts present in a medium sand-size matrix (Figure 13B). Sorted sandstones are typically found overlying basement at the nonconformity contact (Figure 5A and 5C).

In one slab, a massive conglomerate/pebbly sandstone, composed primarily of basalt clasts, grades vertically into a granule conglomerate followed by a medium grained sandstone with rare pebbles. The bed thickness is 8 cm. Overall, clast size is reduced vertically.

Interpretation

The sorted sandstone and conglomerate facies may have been produced by a wide spectrum of hydrological processes that range from hyperconcentrated flows generated during sheet wash events to normal stream flows.

The rounding and sorting of both granitic and basaltic clasts indicates that some fluvial transport took place. Both conglomerates and sandstones are characterized by the absence of well-developed stratification. Grain deformation is minimal in this facies and grain size is easily identifiable in both slabs and thin sections, therefore the absence of stratification is mostly likely primary and not structural.

Sand- and granular-rich hyperconcentrated flows produce deposits which lack distinctive cross-stratification or ripple deposits. These deposits are generally poorly sorted and massive or with rare vague horizontal stratification (Nemec and Muszynski, 1982; Wells, 1984; Smith 1986; Smith and Lowe, 1991). In contrast to these hyperconcentrated-flow deposits found in more recent settings, this facies is finer grained and is better sorted. This discrepancy in grain size and sorting may be attributed to the extensive grusification that occurred in the source area. The grusification processes will most often produce granular size or smaller detritus with the odd larger clast. This limits a size of the sediment delivered into the depositional system.

Hyperconcentrated flows may develop by dilution of debris flows or by sediment bulking (Rodolfo and Arguden, 1991). In the Catoctin Formation setting, hyperconcentrated flows

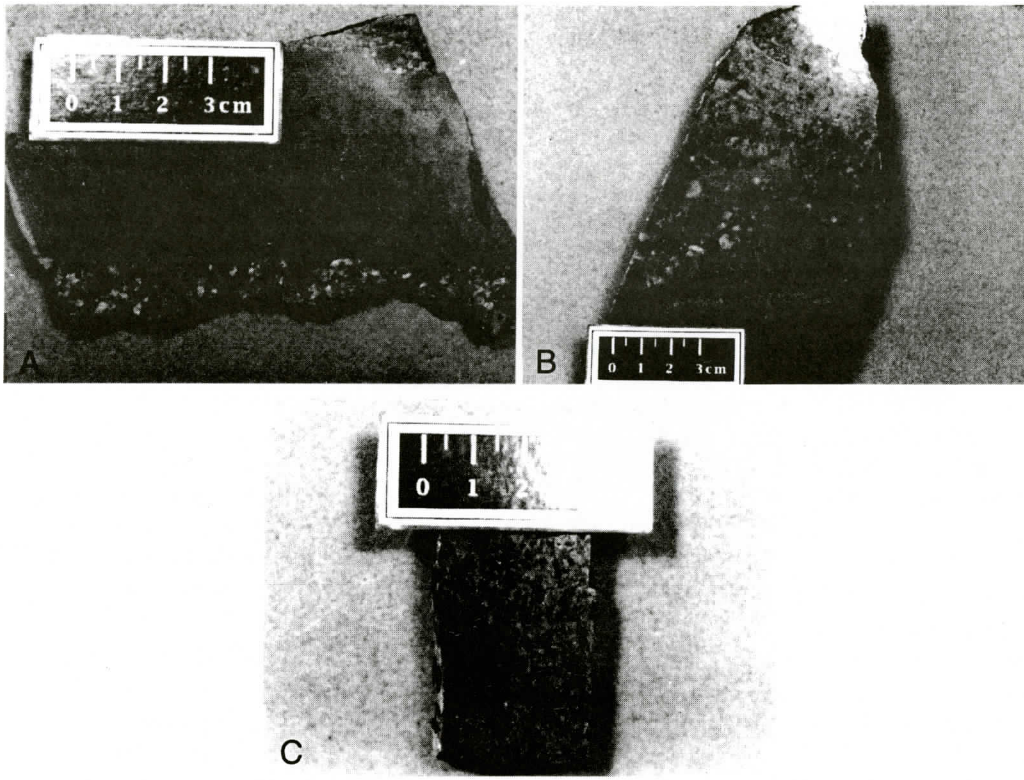

Figure 13. Photographs of sorted sandstone and siltstone facies. A) Massive medium grained sandstone resting on SMCS contact. Note the mudstone ripped up chips. B) Clast-supported conglomerate with minor component of basalt clasts above a medium-grained pebbly sandstone. C) Massive coarse-grained sandstone.

were most likely generated by sediment bulking, addition of sediment to the flow by bed erosion, derived from underlying colluvial deposits, or dilution of debris flows. Colluvial deposits may evolve into debris flow upon movement down slope (Blair and McPherson, 1994a). The recognition of debris flows associated with the inlier is problematic, so direct development from debris flows is an unproven mechanism. The bulking by erosion of colluvial deposits is supported by the evidence of traction reworking in the breccia facies.

The presence of fining-upward sequences consisting of conglomerates passing into sorted sandstones indicates a dominance of more normal, hydraulic conditions. Massive conglomerate-sandstone beds are best interpreted to be deposited from fluvial systems.

The petrology of the sediments within this facies indicates that two areas contributed sediment to the fluvial system. The common occurrence of basalt clasts most likely results from erosion and transport of detritus basalt deposits. Eruption of lava flows into a fluvial system displaces and disrupts local drainage patterns to the periphery of flows, most likely to the edge of the flood plain (Smith, 1988; Inbar and others, 1995). The displacement of channels towards the elevated area would increase the probability of reworking colluvial material by the valley drainage. An axial-valley drainage component of the sediment is supported by the well-sorted and rounded sandstones, which required a significant transport distance. Sorted sandstones were also observed between basalt flows adjacent to the inlier location. Additionally, in proximity to Big Meadows, Badger (1986; 1992) reported ripple cross-laminated sand-

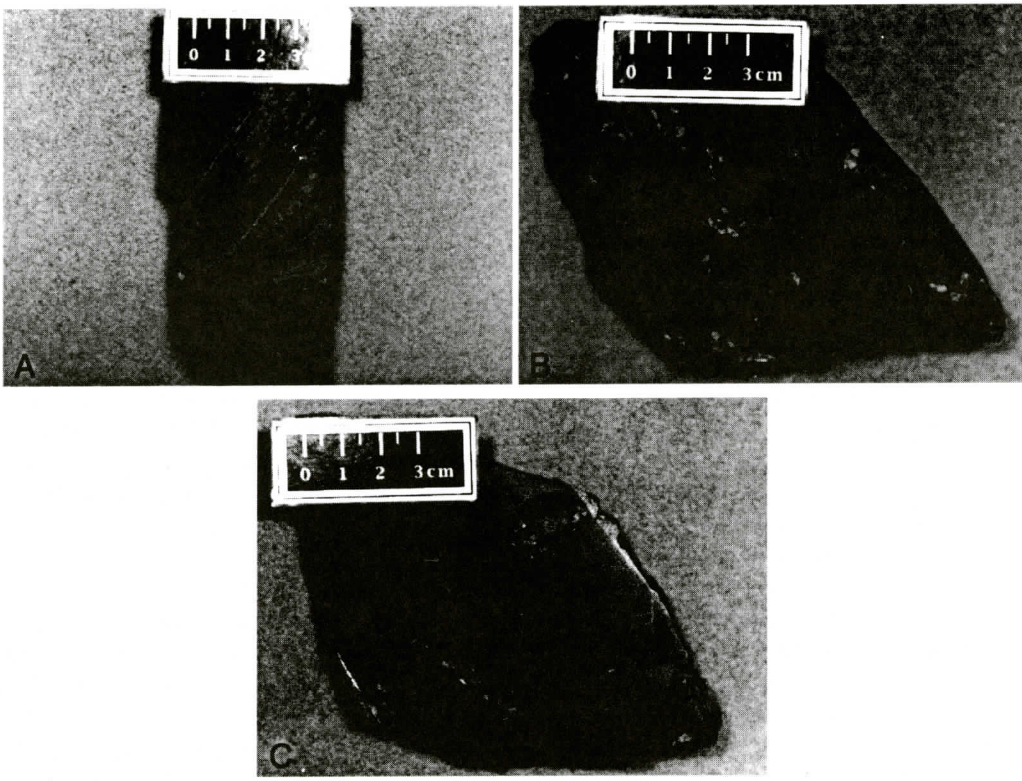

Figure 14. Photographs of the soft-sediment deformed heterolithic facies. A) Deformed laminations of sandstone and siltstone. Note the difference in orientation of laminations, lateral change in thickness and brittle syndepositional faults near top of slab. B) Pebbly mudstone and sandstone. Dark colored clast in the center is red mudstone encased in medium- to fine-grained sandstone. Note the irregular contact between the sandstone and mudstone.

stones separating basalt flows. Sorted sandstones between flows found away from the paleosurface indicates that valley drainage was not always restricted to the periphery and that drainage at times was reestablished on flow tops. The estimated time for drainage development to be established across tops of basalt flows in the Cima volcanic dome field, California, was on the scale of a few thousands years (Dohrenwend and others, 1987). Therefore, an apparent lack of deposits from well-developed fluvial systems between basalt flows in the study area is best explained by high eruption frequency of flood basalts.

Soft-sediment Deformed Heterolithic Facies

Description

The soft-sediment deformed heterolithic facies is composed of lithologies that vary from sandstones to mudstone, all of which display some degree of soft-sediment deformation (Figure 14A-C). This facies is the least common of the three. Two distinctive rock types are recognized, graded laminations consisting of coarse sandstone and siltstone (Figure 14A) and pebbly mudstone and sandstone (Figure 14B and 14C).

The graded laminations of coarse sandstone to siltstone display folding; small-scale normal faults offset folded laminations (Figure 14A). Sands are thickened into the center of the antiforms.

The pebbly mudstone and sandstone contain angular, tabular pebble-size clasts of granite and red mudstone (Figure 14B and 14C). These clasts are encased in a swirled matrix of sand and mud layers. The transition from the contorted, swirled layer are marked by the presence of load and flame structures. Additionally, red mudstone clasts contain features that suggest soft-sediment injection of the surrounding sand into the edge of the clasts. In graded laminations of sand and siltstone, the transition from the siltstone into the overlying sandstone bed is delimited by load and flame structures.

Interpretation

The soft-sediment deformed heterolithic facies may have accumulated in a wide spectrum of depositional settings, but this facies is best interpreted as deformed lacustrine deposits. Damming of river drainage by lava flows is a common occurrence in volcanic settings (Cas and Wright, 1988; Inbar and others, 1995). The variation of the sediment size in the graded laminations consisting of coarse sandstone (Figure 14A) and siltstone is interpreted as the result of variations in sediment inflow to the lake. Inbar and others (1995) report that lacustrine deposits generated by lava damming are well laminated and that these lakes may be subsequently drained by incising fluvial systems. Lacustrine settings would be the sites of high water tables and increase the likelihood of soft-sediment deformation. The presence of lacustrine environments associated with the basaltic flows is also supported by the presence of a limited number of pillow basalts (Badger, 1992).

The large angular pebble-size clasts of granite or red mudstone that is encased in the swirled mixture of sand to mud layers may record deposition from a muddy debris flow on a flood plain or soft-sediment deformation in a lacustrine setting. Colluvium moving down slope may evolve into a debris flow (Blair and McPherson, 1994a). This debris flow may have runout over the lacustrine or overbank deposits incorporating them into the flow. Clasts within the pebbly mudstone are sporadic and in conjunction with the development of extensive granular colluvial deposits that lack mud, a lacustrine or floodplain interpretation is more probable.

According to Mills (1983), mechanisms that produce soft-sediment deformation include liquefaction or fluidization, reverse density gradation, slumping or slope failure, shear stress or a combination of several mechanisms. These mechanisms can be generated in diverse depositional settings. If these lacustrine deposits were covered by an erupting lava flow then soft-sediment deformation could easily be induced. The water-saturated condition would increase the pore pressure resulting in increased fluidization potential. Additionally, deposition was taking place in an active tectonic setting that was probably subjected to earthquakes.

DISCUSSION

The preservation of the paleotopography and the genetic relationship between the paleotopography, clastics deposits and volcanic rocks are examined below (Figure 15).

The Swift Run Formation, typically, is preserved as valley fills within its westernmost outcrops (Gathright, 1976), whereas, the Swift Run Formation towards the east is a more continuous tabular unit (Gathright, 1976; Bartholomew, 1977; Gathright and others, 1977). This difference in geometry is best related to the distribution of the preserved paleotopography; eastern Swift Run Formation accumulated in a broad low-relief valley or basin (Figure 15 top), whereas the western deposits accumulated in areas characterized by relatively high relief topography (Gathright, 1976). Bartholomew and others (1981) and Bartholomew (1992) document of the westward pinchout of the Catoctin Formation as determined from maps and cross sections.

Speculatively, the broad valley may have developed during extension. The western side of the basin was incised by streams that delivered detritus to basin. As extension continued, volcanism increased and progressively infilled the basin and onlapped the basement topography (Figure 15 bottom). The northeastward tilt of the reconstructed paleosurface does not reflect the orientation of a tectonic structure, but an

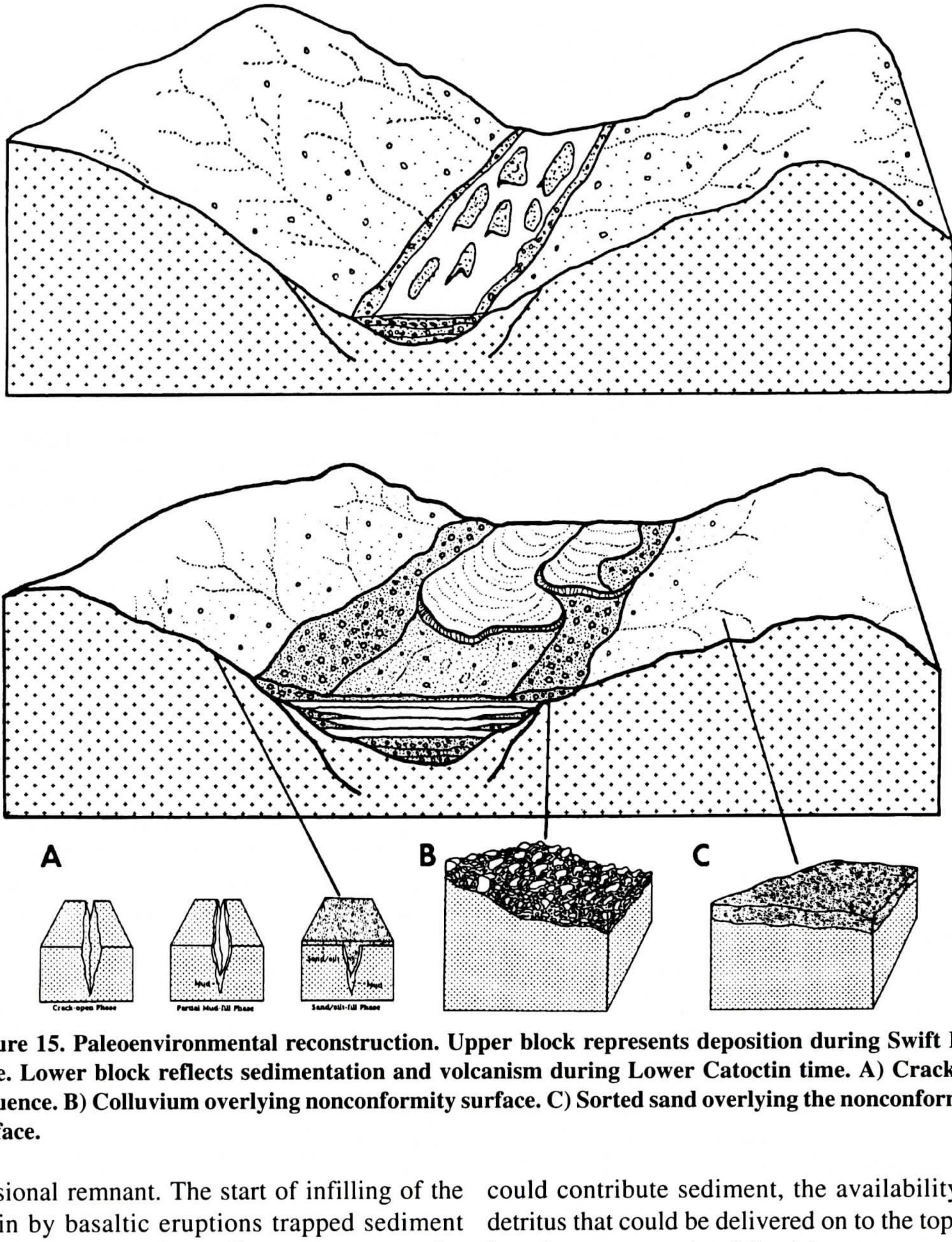

Figure 15. Paleoenvironmental reconstruction. Upper block represents deposition during Swift Run time. Lower block reflects sedimentation and volcanism during Lower Catoctin time. A) Crack fill sequence. B) Colluvium overlying nonconformity surface. C) Sorted sand overlying the nonconformity surface.

erosional remnant. The start of infilling of the basin by basaltic eruptions trapped sediment within the extensive valley system near the footwall, starving the basin center of detritus. Dilliard and others (in press) identified only small channel-shaped sandstone bodies occurring within the lower part of the Catoctin Formation to the south of Big Meadows. Progressive covering of the sediment in the valleys by basalt flows permitted only exposed paleohighs to be the source for sediments (See Bartholomew, 1977). Although the paleohigh could contribute sediment, the availability of detritus that could be delivered on to the tops of lava flows or associated fluvial systems was reduced by burial.

At a high southern latitude, the exposed Mesoproterozoic basement was subjected to grusification. Meert and Van der Voo (1992) report a high southern latitude pole from the Catoctin Formation. Park (1994) examining recent paleomagnetic results from the Neoproterozoic-age strata from the western Cordillerion region supports a southern high latitude for the accumulation of the Catoctin basin. A high-latitude position would have promoted a decrease rate of chemical weathering and enhanced grusification. Extensive soil development at these high latitudes would have been inhibited which explains the lack of reported extensive paleosols. Additionally, the high latitude climate would have produced relatively little clay from weathering of the granites and basalts, supported by a general paucity of mudstone in the Catoctin Formation (Dilliard and others, in press).

Blair and McPherson (1994a; 1994b) recognize different stages associated with the development of alluvial fans. Each stage is characterized by a successive reduction in slope and a change in sedimentary processes. According to their developmental scheme, colluvial slope failure deposits are commonplace in the early stages. In the study area, however, the development of mature extensive alluvial fans on the margins of the Catoctin basin was probably inhibited by basalt flows covering the alluvial fan or restricting sediment supply to the periphery of the valley. In these lateral positions, colluvium could then be reworked and transported by normal stream flow processes.

CONCLUSIONS

An inlier through the Catoctin Formation exposes Grenville- age charnockite, in stream cuts near Big Meadows, Shenandoah National Park, VA. The study of the inlier contact, a nonconformity, and onlapping relationship of sediments and basalts provides an opportunity to gain insight into the characteristics of the paleotopography and development of adjacent fluvial systems. The contact elevation is corrected for the local structure and new elevations are contoured. The gradient of this currently north-facing slope is calculated to be ~20% or 11 degrees. Using a distinctive porphyritic basalt flow, the minimum relief from the lowermost basalt flow to the top surface of the inlier is determined to be ~180 meters. The charnockite beneath the nonconformity surface is in sharp contact with either sediment or basalt. No soil horizons are identified and probably did not develop due to the high gradient of the nonconformity surface. In some areas, the SMCS surface is characterized by cracks infilled with siltstone and fine-grained sandstone. Crack dimensions average 1.5 cm in width with variable lateral continuity. Some cracks record complex sediment and basalt infill histories. Sediment deposits, associated with the paleotopography, contain granite and subordinate basalt clasts. Deposits range from very angular and poorly sorted breccia to rounded and sorted sandstone. The breccia is considered to represent colluvium that washed off the steep granodiorite highs. Breccias containing intermixed basalt clasts reflect minor reworking of the granitic colluvium by fluvial processes and intermixing of basalt clasts derived from a distant source. The sorted sandstones indicate significant fluvial reworking of the colluvial material. The soft-sediment deformed heterolithic facies most likely records deposits in a flood plain or lacustrine setting.

ACKNOWLEDGEMENTS

We thank Jerry Bartholomew and Kathleen Farrell for their careful and complete reviews. Mike Wizevich critically reviewed an earlier version of this paper. Fieldwork was supported by professional development grants from the Pennsylvania State System of Higher Education to ES. Thanks to Dave Anastasio for use of his photographic microscope. We are grateful to the staff of Shenandoah National Park for providing access and collecting permits

REFERENCES CITED

Aleinikoff, J.N., Zartman, R.E., Walter, M., Rankin, D.W., Lyttle, P.T., and Burton, W.C., 1995, U-Pb ages of metarhyolites of the Catoctin and Mount Rodgers formations, central and southern Appalachians: evidence for two pulses of Iapetan rifting: American Journal of Science, v. 295, p. 428-454.

Badger, R.L., 1986, Stratigraphy of the Catoctin volcanic province, central Appalachians, *in* Harding, L.E., and Coney, P.J., editors, A Collection of Papers Honoring Brewster Baldwin: Middlebury College, Middlebury, Vermont, p. 1-14.

Badger, R.L., 1992, Stratigraphic characterization and correlation of volcanic flows within the Catoctin Formation, central Appalachians: Southeastern Geology, v. 32, p. 175-195.

Badger, R.L., and Sinha, A.K., 1988, Age and Sr isotopic signature of the Catoctin volcanic province: Implications of subcrustal mantle evolution: Geology, v. 16, p. 692-695.

Bartholomew, M.J., 1977, Geology of the Greenfield and Sherando Quadrangles, Virginia: Virginia Division of Mineral Resources, Publication No. 4, p. 11-16.

Bartholomew, M.J., 1992, Structural characteristics of the Late Proterozoic (post-Grenville) continental margin of the Laurentian craton, *in* Bartholomew, D. W., and others, editors, Characterization of comparison of ancient and Mesozoic Continental Margins — Proceedings of the 8th International Conference on Basement Tectonics: Kluwer Academic Publishers, Netherlands, p. 443-467.

Bartholomew, M.J., and Lewis, S.E., 1984, Evolution of Grenville massifs in the Blue Ridge geologic province, southern and central Appalachians, *in* Bartholomew, M. J., and others, editors, The Grenville event in the Appalachians and related topics: Geological Society of America, Special Paper 194, p. 229-254.

Bartholomew, M.J., Gathright, T.M. II, and Henika, W. S., 1981, A tectonic model for Blue Ridge in central Virginia: American Journal of Science, v. 281, p. 1164-1183.

Battiau-Queney, Y., 1996, A tentative classification of paleoweathering formations based on geomorphic criteria: Geomorphology, v. 16, p. 87-102.

Blair, T.C., and McPherson, J.G., 1994a, Alluvial fans and their natural distinction from rivers based on morphology, hydraulic processes, sedimentary processes, and facies assemblages: Journal of Sedimentary Research, v. A64, p. 450-489.

Blair, T.C., and McPherson, J.G., 1994b, Alluvial fan processes and forms, *in* Abrahams, A.D., and Parsons, A.J., editors, Geomorphology of Desert Environments: London, Chapman and Hall, p. 354-402.

Bovis, M.J., 1986, The morphology and mechanics of large-scale slope movements, with particular reference to southwest British Columbia, *in* Abrahams, A. D., editor, Hillslope Processes: Boston, Allen and Unwin, p. 319-341.

Caine, N., 1980, The rainfall intensity-duration control of shallow landslides and debris flows: Geografiska Annaler, v. 64A, p. 23-27.

Cronin, V.S., 1992, Compound landslides: nature and hazard potential of secondary landslides within host landslides, *in* Slossen, J.E., Kene, A.G., and Johnson, J.A., editors, Landslides/Landslide Mitigation: Geological Society of America Reviews in Engineering Geology: No. 9, p. 1-9.

Cas, R.A.F., and Wright, J.V., 1988, Volcanic Successions Modern and Ancient: Unwin Hyman, London. 528 p.

deVillers, A.B., 1989, The fossil landscape of the Vredefort dome: Zeitschrift für Geomorphologie N. F., v. 33, p. 93-101.

Dilliard, K.A., Simpson, E.L., Noto, R.C., and Wizevich, M., in press, Characterization of fluvial deposits interbedded with flood basalts, Neoproterozoic Catoctin Formation, central Appalachians, U.S.A.: Precambrian Research.

Dohrenwend, J.C., Abrahams, D., and Turrin, B.D., 1987, Drainage development on basaltic lava flows, Cima volcanic field, southeast California, and Lunar crater volcanic field, south-central Nevada: Geological Society of America Bulletin, v. 99, p. 405-413.

Eggler, D.H., Larson, E.E., and Bradley, W.C., 1969, Granites, grusses, and the Sherman erosion surface, Southern Laramie Range, Colorado-Wyoming: American Journal of Science, v. 267, p. 510-522.

Ellen, S.D., and Flemming, R.W., 1987, Mobilization of debris flows from soil slips, San Francisco Bay region, California, *in* Costa, J.E., and Wieczorek, G.F., editors, Debris Flows/Avalanches: Process, Recognition and Mitigation: Geological Society of America Reviews in Engineering Geology, v. 7, p. 31-40.

Fahey, B.D., 1985, Salt weathering as a mechanism of rock breakup in cold climates: An experimental approach: Zeitschrift für Geomorphologie N. F., v. 29, p. 99-111.

Fairbridge, R.W., and Finkl, C.W., Jr., 1980, Cratonic erosional unconformities and peneplains: Journal of Geology, v. 88, p. 69-86.

Folk, R.L., and Patton, E.B., 1982, Buttressed expansion of granite and development of grus in Central Texas: Zeitschrift für Geomorphologie N. F., v. 26, p. 17-32.

Gardner, J.S., 1983, Accretion rates on some debris slopes in the Mt. Rae area, Canadian Rocky Mountains: Earth Surface Processes and Landforms, v. 8, p. 347-355.

Gathright, T.M., 1976, Geology of the Shenandoah National Park, Virginia: Virginia Division of Mineral Resources, Bulletin no. 86. 93 p.

Gathright, T.M., Henika, W.S., and Sullivan, J.L., III, 1977, Geology of the Waynesboro East and Wanyesboro West quadrants, Virginia: Virginia Division of Mineral Resources, Publication No. 3, 53 p.

Hughes, S.S., Lewis, S.E., Bartholomew, M.J., Sinha, A.K., Hudson, T.A., and Herz, N., 1997, Chemical diversity and origin of Precambrian charnockitic rocks of the central SMCS massif, Grenville Blue Ridge Terrane, Virginia: Precambrian Research, v. 84, p. 37-62.

Inbar, M., Risso, C., and Parica, C., 1995, The morphological development of a young lava flow in the South Western Andes - Neuquen, Argentina: Zeitschrift für Geomorphologie N. F., v. 39, p. 479-487.

Isherwood, D., and Street, A., 1976, Biotite-induced grusification of the Boulder Creek Granodiorite, Boulder County, Colorado: Geological Society of America Bulletin: v. 87, p. 366-370.

Keefer, D.K., 1984, Landslides caused by earthquakes: Geological Society of America Bulletin, v. 95, p. 406-421.

Meert, J.G., and Van der Voo, R., 1992, Evidence for a high paleolatitude of North America in the latest Precambrian and rapid drift during the Cambrian: EOS, v. 73, p. 150.

Mills, H.H., 1987, Variation of sedimentary properties of colluvium as a function of topographic setting, Valley and Ridge province, Virginia: Zeitschrift für Geomorphologie N. F., v. 31, p. 277-292.

Mills, P.C., 1983, Genesis and diagnostic value of soft-sediment deformation structures ñ a review: Sedimentary Geology, v. 35, p. 83-104.

Narbonne, G.M., 1998, The Ediacara biota: A terminal Neoproterozoic experiment in the evolution of life: GSA Today, v. 8, No. 2, p. 1-6.

Nemec, W., and Muszynski, A., 1982, Volcaniclastic alluvial aprons in the Tertiary of Sofia District (Bulgaria): Annales Societatis Geologorum Poloniaz, v. 52, p. 239-303.

Ollier, C.D., Gaunt, G.F.M., and Jurkowski, I., 1988, The Kimberly Plateau, Western Australia, a Precambrian erosion surface: Zeitschrift für Geomorphologie N. F., v. 32, p. 239-246.

Park, J.K., 1994, Palaeomagnetic constraints on the position of Laurentia from the middle Neoproterozoic to Early Cambrian times: Precambrian Research, v. 69, p. 95-112.

Rankin, D.W., compiler, 1993, Map A geological map of Precambrian (Proterozoic) rocks east of the Grenville front and their geological setting in the United States and adjacent Canada, *in* Hatcher, R.D. Jr., Thomas, W.A. and Viele, G.W., editors, The Appalachian-Ouachita Orogen in the United States: Plate 5.

Reed, J.C., Jr., 1955, Catoctin Formation near Luray, Virginia: Geological Society of America Bulletin, v. 66, p. 871-896.

Reed, J.C., Jr., 1969, Ancient lavas in Shenandoah National Park near Luray, Virginia: United States Geological Survey Bulletin, No. 1265: 43 p.

Reed, J.C., Jr., and Morgan, B. A., 1971, Chemical alteration spilitization of the Catoctin Greenstones, Shenandoah National Park, Virginia: Journal of Geology, v. 79, p. 526-548.

Reneau, S., Dietrich, W.E., Donahue, D.J., Jull, A.J.T., and Rubin, M., 1990, Late Quaternary history of colluvial deposition and erosion in hollows, central California Coastal Ranges: Geological Society of America Bulletin, v. 102, p. 969-982.

Rodolfo, K.S. and Arguden, T., 1991, Rain-lahar generation and sediment-delivery systems at Mayon Volcano, Philippines, *in* Fisher, R.V., and Smith, G.A., editors, Sedimentation in Volcanic Settings: Society of Economic Paleontologists and Mineralologists No. 45, p. 72-87.

Simpson, E.L., and Eriksson, K.A., 1989, Sedimentology of the Unicoi Formation in southern and central Virginia: evidence for late Proterozoic to Early Cambrian rift-to-passive margin transition: Geological Society of America Bulletin, v.100, p. 42-54.

Smith, G.A., 1986. Coarse-grained nonmarine volcaniclastic sediment: terminology and depositional process: Geological Society of America Bulletin, v. 97, p. 1-10.

Smith, G.A., 1988, Neogene synvolcanic and syntectonic sedimentation in central Washington: Geological Society of America Bulletin, v. 100, p. 1479-1492.

Smith, G.A., and Lowe, D.R., 1991, Lahars: volcano-hydrologic events and deposition in the debris flow-hyperconcentrated flow continuum, *in* Fisher, R.V., and Smith, G.A., editors, Sedimentation in Volcanic Settings: Society of Economic Paleontologist and Mineralogists Special Publication No. 45, p. 59-70.

Smith, N., and Bishop, P., 1993, The use of palaeo-flow direction indicators in basaltic lavas in landscape history reconstruction: A reconnaissance study and evaluation from northern New South Wales, Australia: Zeitschrift für Geomorphologie N. F., v. 37, p. 157-170.

Taylor, G., Taylor, G.R., Bink, M., Foudoulis, C., Gordon, I., Hedstrom, J., Minello, J., and Whippy, F., 1985, Pre-basaltic topography of the Northern Monaro and its implications: Australian Journal of Earth Sciences, v. 32, p. 65-71.

Tollo, R.P., and Aleinikoff, J.N., 1996, Petrology and U-Pb geochronology of the Robertson River igneous suite, Blue Ridge province, Virginia - evidence for multistage magmatism associated with an early episode of Laurentian rifting: American Journal of Science, v. 296, p. 1045-1090.

Tollo, R.P., and Hutson, F.E., 1996, 700 Ma age for the Mechum River Formation, Blue Ridge province, Virginia: A unique time constraint on pre-Iapetan rifting of Laurentia: Geology, v. 24, p. 59-62.

Twidale, C.R., 1976, On the survival of paleoforms: American Journal of Science, v. 276, p. 77-95.

Twidale, C.R., 1997, Tectonic regime and preservation of palaeosurfaces: Zeitschrift für Geomorphologie N. F., v. 41, p. 479-490.

Unrug, R., 1997, Rodinia to Gondwana: The geodynamic map of Gondwana Supercontinent assembly: GSA Today, v. 7, p. 1-6.

Varnes, D.J., 1978, Slope movement types and processes, *in* Schuster, R.L., and Krizek, R.J., editors, Landslides, Analysis and Control: Washington, D.C., Transportation Research Board, National Academy of Sciences, Special Report 176, p. 11-33.

Wehr, F., and Glover, L. III, 1985, Stratigraphic and tectonics of the Virginia-North Carolina Blue Ridge: evolution of a late Proterozoic hinge zone: Geological Society of America Bulletin, v. 96, p. 285- 295.

Wells, N.A., 1984, Sheet debris flow and sheetflood conglomerates in Cretaceous cool- marine alluvial fans, South Orkney Islands, Antarctica, *in* Koster, E.H., and Steel, E.J., editors, Sedimentology of Gravels and Conglomerates: Canadian Society of Petroleum Geology Memoirs, No. 10, p. 133- 145.

Whalley, W.B., Douglas, G.R., and McGreevy, J.P., 1982, Crack propagation and associated weathering of igneous rocks: Zeitschrift für Geomorphologie N. F., v. 26, p. 33-54.

Wielemaker, W.G., and van Dijk, G.R., 1981, Mapping and correlation of erosion surfaces, variously affected by volcanic ash, tectonism and lava flows - a case study in S. W. Kenya: Zeitschrift für Geomorphologie N. F., v. 25, p. 54-72.

SOUTHEASTERN GEOLOGY
V. 38, No. 4, August 1999, p. 259-278

Regional Facies Analysis and Carbonate Ramp Development in the Tonoloway Limestone (U. Silurian; Central Appalachians)

S.C. Bell

13016 National Pike, Clear Spring, MD 21722

R. Smosna

Dept. of Geology and Geography, West Virginia University, Morgantown, WV 26506

ABSTRACT

A comprehensive facies model of the Tonoloway Limestone shows an array of depositional environments from carbonate lagoon-sabkha on the NNE to deeper ramp on the SSW. This model is significant to the developmental history of the central Appalachian basin because carbonate-ramp facies have not been previously recognized in the pre-Helderberg part of the Upper Silurian interval.

Four regional facies-environments are recognized: Carbonate Lagoon-Sabkha, Sandy Lagoon-Sabkha, Shallow Ramp, and Deep Ramp-Tempestites. In the carbonate lagoon, moderate to low energy, skeletal/oolitic sand flats passed landward into subtidal mudflats, muddy intertidal flat, and sabkha. Conditions varied from restricted to open-marine, and depths were everywhere above wave base (15 m). The minor Sandy Facies (including the Indian Springs Sandstone Member) represent quartz-rich counterparts to the restricted carbonate lagoon-sabkha.

The shallow ramp consisted of high-energy crinoid shoals and deeper, offshoal biostromes, floatstone/wackestone/packstone, and nodular lime sediments. Frame builders included stromatoporoids, bryzoans, and corals. Maximum depth was between normal wave base (15 m) and storm wave base (40 m). Graded carbonate tempestites formed on the deep ramp, where water depths reached storm wave base. Open-marine conditions prevailed on both parts of the ramp.

The lagoon/sabkha-shallow ramp-deep ramp profile existed during the middle of Tonoloway time and extended from Pennsylvania through Maryland, Virginia, and West Virginia, with the ramp sloping gently S. The ramp developed from a regional epeiric platform coincident with a northeastward transgression between two regressions, all within the 1-3 Ma total span of Tonoloway time. Both eustatic activity and tectonic mechanisms, possibly related to basement-fault reactivation, acted as controls on ramp development.

INTRODUCTION AND BACKGROUND

The Tonoloway Limestone records a significant part of the thick succession of Siluro-Devonian carbonates in the central Appalachian basin, but facies studies are presently available only from the northern part of the outcrop belt. Furthermore, it has been popularly inferred from these localized studies that the Tonoloway depositional system was simply a coastal sabkha bordering an epeiric seaway throughout its history. A series of massive and coarse-grained limestones, however, throughout the southern part of the outcrop belt in West Virginia and Virginia suggests that a strikingly different carbonate setting existed there during much of Tonoloway time. The origin of those limestones, interpreted here as ramp deposits, and their relationship to other Tonoloway facies have not been previously studied. The purpose of this paper, therefore, is to produce the first comprehensive, regionally complete facies-environment analysis of the Tonoloway Limestone. The main objectives are: 1) identify all depositional facies represented in the Tonolo-

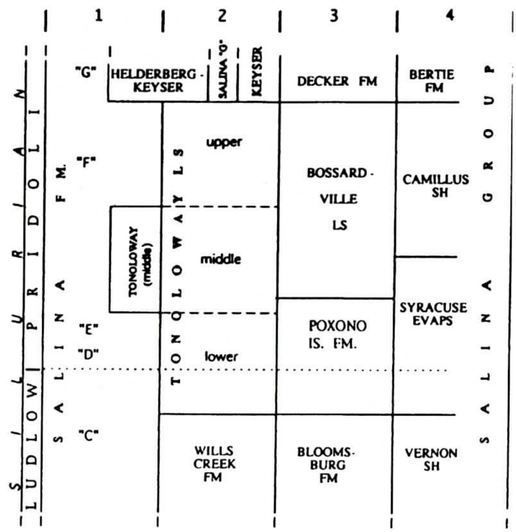

Figure 1. Stratigraphic relationships in and around the central Appalachian Basin during the uppermost Ludlow and Pridoli, showing the Tonoloway Limestone and equivalents. Column numbers correspond to numbered areas in Figure 2. References: Patchen and others (1984); Smosna et. al. (1977); Dennison (1970); Head (1969).

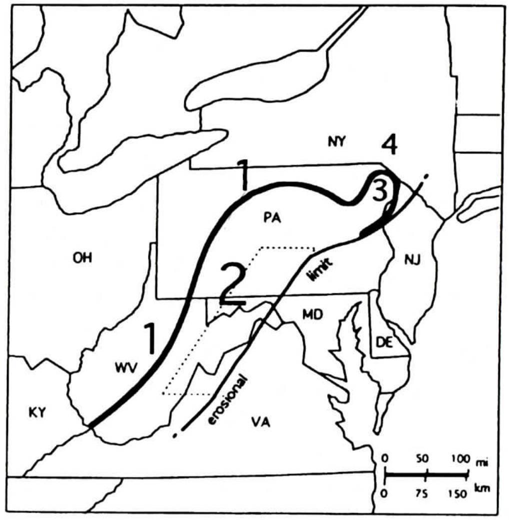

Figure 2. Regional map showing the limits of the Tonoloway Limestone (heavy line) and location of the study area (dotted line), which lies within the outcrop belt. The eastern limit is the erosional limit of the Silurian. Numbered areas correspond to numbered stratigraphic columns in Figure 1.

way outcrop belt and provide a comprehensive set of descriptions and environmental interpretations, 2) provide a regional-scale correlation of the major facies-environments, and 3) by integrating our results, produce a model showing the regional array of facies, water depths, and depositional settings. Tectonic versus sea-level control on the development of the ramp is discussed as a special salient matter at the end. This study represents the first documentation of the ramp facies, and it provides the necessary foundation for a sequence-stratigraphic analysis of the Tonoloway, planned by the authors for publication in the near future.

The Tonoloway carbonate facies belt is bordered by evaporite-dolomite facies (Salina Formation) on the west and siliciclastic facies (Poxono Island Formation, Camillus Shale) on the northeast (see Figures 1, 2). It is regionally underlain by the Wills Creek Formation and overlain by the Siluro-Devonian Helderberg Group. Based on conodont zonation, the time represented by the Tonoloway encompasses the latest Ludlow and first half of the Pridoli (Helfritch,1975; Berry and Boucot, 1970). Using a range of two to six million years for the total length of the Pridoli (Harland and others, 1982; Palmer, 1983; McKerrow and others,1985; Salvador, 1985), it is estimated that the Tonoloway formed over a period of 1-3 million years.

Woodward (1941) informally subdivided the Tonoloway into lower, middle, and upper members, and various workers have since used this three-part subdivision throughout the region. The upper and lower members are characterized by abundant thin bedding and lamination, muddy texture, frequent dolomitic beds, an abundance of evaporite features, the presence of siliciclastics, and a fauna composed mainly of ostracodes. In the northern part of the region, the middle member is characterized by thicker beds, more limestone, and significantly greater weathering resistance. Faunal diversity is also usually higher. In the southern area, Woodward's (1941) middle member stands out as an interval of massive and coarse-grained limestone with a highly diverse and abundant fauna. Smosna and others (1977) correlated the three members regionally and into the subsurface beneath the Alleghany Plateau to the west. In the present study, these members provide an informal framework helpful in deciphering the regional lithofacies pattern.

Earlier facies studies were concentrated in the classic Tonoloway outcrop area surrounding the Potomac River. Using sections measured in that area, Tourek (1970) interpreted the combined Wills Creek-Tonoloway Formations as a sabkha-lagoon deposited in an epeiric seaway under arid conditions. Facies recognized by that study were discussed in petrographic detail, but they are relatively difficult to differentiate in outcrop. Based on thin sections from the outcrop at Pinto, Md., Smosna and others. (1977) recognized a series of three peritidal depositional environments transitional in terms of water depth, hydrodynamic energy, and fossil diversity: supratidal-intertidal; shallower, higher-energy subtidal; and deeper, lower energy subtidal. Smosna and Warschauer (1979) later subdivided that depositional model into a total of seven environments. Those studies concluded independently of Tourek (1970) that the Tonoloway seaway fits Irwin's (1965) epeiric model. A later thin-section study by Smosna and Warschauer (1981) at Pinto, Md., refined the classification of supratidal-intertidal zones in terms of relative exposure. No detailed study has been made of either Woodward's (1941) middle member, which represents a distinct southern facies, or of Swartz's (1923) Indian Springs Sandstone Member, which represents a distinct eastern facies.

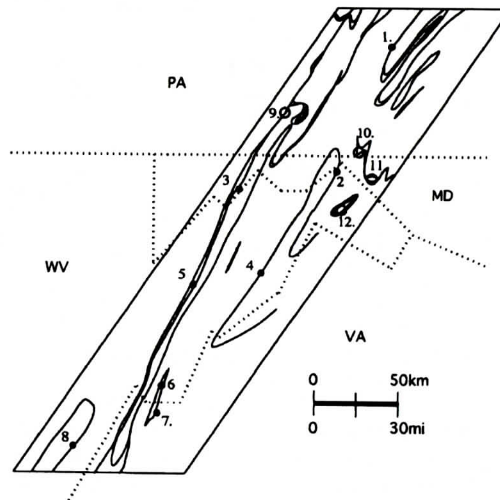

Figure 3. Study area map showing outcrop belts, major outcrop sections used in this study (dots), and auxiliary outcrops (open circles): 1: Allenport, PA; 2: Grasshopper Run, WV; 3: Pinto, MD; 4: McCauley, WV; 5: Powers Hollow, WV; 6: Crummet Run, WV; 7: McDowell, VA; 8: Knapp Creek, WV; 9: Bedford, PA; 10: Warren Point, PA; 11: Lanes Run, MD; 12: Tomahawk, WV.

METHODS AND PROCEDURE

The most complete Tonoloway sections throughout the region were used in this study, which is limited to the outcrop belt due to the poor quality of well data available in the subsurface area to the west. Eight major outcrops and four auxiliary outcrops were chosen and plotted on a regional base map. The study area (Figure 3), defined by the Valley and Ridge Province from central Pennsylvania to southeastern West Virginia, is 400 km long and covers 40,000 sq.km.

Sections were described in detail (approximately at the centimeter scale) on a bed-by-bed basis in the field and sampled for lab analyses, which included examination by binocular microscope, thin-section petrography, and acetate peels. Field and lab data were then used to identify and describe the various lithofacies and facies associations. Depositional environments and subenvironments were interpreted using the sedimentologic data together with the stratigraphic relationships observed among facies. Environmental interpretation was aided by comparison with modern and ancient examples from the literature. Finally, a model was constructed to explain the lateral correlation of major facies on a regional scale.

TONOLOWAY LITHOFACIES, FACIES ASSOCIATIONS, AND DEPOSITIONAL ENVIRONMENTS

The lithofacies and facies associations are described below and interpreted in terms of their depositional environments; this information is summarized in Table 1. Lithofacies names are descriptive and reflect the most

Table 1. Summary of Tonoloway facies, as recognized in this study. Details appear in text.

CARBONATE LAGOON-SABKHA FACIES ASSOCIATION

LAMINITE FACIES

Lithology, Stratification, Features: cryptalg. & mechan. micritic lams; deep polygon mudcracks; mm evap. molds; lam roll-ups.

Interpretation: intertidal carbonate mud flat, unchannelled

DOLOMITE FACIES

Lithology, Stratification, Features: dolo. & dolo. ls: microdolo. mosaics & micrite; thn.-med. beds; evap. molds & vugs; chickenwire struc; mudcracks.

Interpretation: sabkha

BEDDED MUDSTONE FACIES

Lithology, Stratification, Features: thn.-bdd. mechan. mudst. & wkst. w/ sm. amts. clay & microdolo; abt. ostrcds., var. amts. brachs., bryz., crinoids, corals, gastrpds; intercal algal bds; infreq. mudcracks.

Interpretation: subtid.-lwr. intertid. lagoon mudflat

PELOIDAL-OOLITIC FACIES

Lithology, Stratification, Features: 1) thn. couplets of graded skel.-pel. wkst./pkst., clay-rich at top; 2) oolitic skel.-pel. pkst./grst., thn.-med. horz. bds., radial oolites; both 1) & 2) - intercal. algal bds. & foss. as in Bedded Mudstone Facies.

Interpretation: subtidal lagoon: 1) storm-dom. sand-mud flat; 2) offshore skel. sand flat

INTRACLASTIC FACIES

Lithology, Stratification, Features: 1) intraclastic conglomerate, thn.-med.-bdd; 2) ls. breccia w/ leached pores, evap. molds.

Interpretation: 1) transgressive lag; 2) solution breccia

ALGAL FACIES

Lithology, Stratification, Features: stromatolitic and thrombolitic ls. bds. intercal. in other subtid. fac.

Interpretation: algal biostromes, local bioherms

SANDY LAGOON-SABKHA FACIES ASSOCIATION

MIXED CARBONATE-SILICICLASTIC FACIES

Lithology, Stratification, Features: 1) calcar. ss: alt. or mixed lyrs. of fn. qtz. sand/silt & micrite; local burrws, lams, mudcracks; 2) dolo. ss: same as Dolomite Facies, but w/ var. amts. qtz. sand, silt.

Interpretation: 1) subtidal carbonate-siliciclastic lagoon; 2) sandy sabkha

SILICICLASTIC FACIES

Lithology, Stratification, Features: 1) gray ss: gdd. thn. qtz. arenite-muddy siltst. couplets; 2) green siltst: qtz. silt & clay, green, w/compaction feats; 3) red siltst: qtz. silt & mud, red, w/ mudcracks.

Interpretation: 1) subtidal siliciclastic lagoon; 2) subtid.-intertid. mud flat; 3) supratid. mud flat.

SHALLOW RAMP FACIES ASSOCIATION

CRINOIDAL GRAINSTONE FACIES

Lithology, Stratification, Features: v. coarse skel. grst., crinoid-rich, also brachs., bryz., corals, qtz. sand; thick strat. units w/ lg. & sm. x-bddg, hardgrounds.

Interpretation: hi-E skel. shoals, lg.-scale

MIXED-SKELETAL FACIES

Lithology, Stratification, Features: stromatop. framest., crinoid-rich wkst./pkst./floatst., bryz. framest./bafflest; micritic matx.

Interpretation: offshoal/intershoal deposits

NODULAR LIMESTONE FACIES

Lithology, Stratification, Features: skel.-pel. wkst./pkst. nods. & mudst./wkst./clay matx.; microstylo. swarms; ostracds., pelmatoz., brachs, gastrpds.

Interpretation: deep offshoal/intershoal, storm-dom.

DEEP RAMP - TEMPESTITE FACIES

Lithology, Stratification, Features: gdd. thn. units of shelly pkst. w/ micritic, clay-rich lams. at top, vert. brrws., ripple x-lams.

Interpretation: deep ramp storm deposits

abundant and/ or representative lithology included. All except the Dolomite and Sandy Facies are dominated by limestone. Four facies associations are recognized on the basis of outcrop relationships and common lithologic features. Descriptions emphasize primary depositional features; the aim here is to "see through" diagenetic alteration in order to facilitate environmental interpretations. Interpretations are based on pertinent data in the lithologic description, stratigraphic associations, and analogous sediments studied elsewhere.

Carbonate Lagoon-Sabkha Facies Association

The principal facies in this association are the Laminite Facies (intertidal flat), Dolomite Facies (sabkha), and the Peloidal/Oolitic- and Bedded Mudstone Facies (subtidal lagoon).

Laminite Facies

This is probably the most common facies and consists of flat- to slightly undulose-laminated, mudcracked limestone (Figure 4.A). Laminae are up to 1.0 cm thick and consist of alternating pelleted lime mud layers and dark layers containing thin cryptalgal laminations and micron-scale euhedral dolomite. Mudcracks are often well developed hexagonal polygons up to 1.0 m deep that increase in frequency toward the tops of bedsets. Other features include lamination roll-ups, thicker mudstone/ wackestone layers, thin LLH stromatolites, and thin intraclast layers. Evaporite molds appear confined to narrow intervals toward the tops of lamination sets. Trace amounts of gypsum and anhydrite were observed in samples from the Pinto section (Smosna and Warschauer, 1979).

This facies was deposited on a low-energy, unchannelled carbonate intertidal flat which developed under arid to partly arid conditions. The upper part of the intertidal flat was covered by layered algal (cyanobacterial) mats. Mechanical lime mud laminations formed on the lower part of the flat and were probably stabilized by very thin algal layers. Similar intertidal laminites have been described in Late Cambrian Appalachian carbonates (cf. Osleger and Read, 1991). During storms, lime mud and shell material were washed onto the flat and deposited in slightly thicker layers. Partly lithified or algal-stabilized layers were rolled up by currents or ripped up and re-deposited as thin intraclast layers at some locations. Deep dessication cracks formed under repeated exposure to arid conditions. In the Persian Gulf region, analogous tidal flats are covered by extensive algal mats, which have a higher preservation potential in arid climates where elevated salinities preclude grazing organisms. Gypsum precipitation occurs today under hypersaline conditions in the lower-sabkha/ upper intertidal transition zone of the Persian Gulf (Kinsman, 1964), and that zone is apparently recorded in the Tonoloway by the narrow zones of evaporite molds.

Dolomite Facies

Well bedded dolomite and dolomite-limestone constitutes this facies (see Figure 4.A). Beds weather chacteristically yellow-gray, and some weather quite shaly. Intercalated layers may include stromatolitic laminae, thin layers of ostracode packstone, laminae of quartz silt to very fine sand, and thin layers of granule-size intraclasts. Dolomite beds consist of mosaics of 10-20 μ, anhedral cloudy dolomite associated with micrite. The dolomite-limestone contains scattered euhedral dolomite crystals up to 60 μ in a micritic matrix. At Pinto, Smosna and Warschauer (1979) reported traces of anhydrite and clay minerals (illite and kaolinite) constituting up to 7-9% of the rock. Other features may include evaporite molds, horizontal sheet cracks (Tourek, 1970), discoid vugs, small mudcracks, and rare poorly-preserved "chickenwire" structure. This facies is usually underlain by the Laminite Facies.

The Dolomite Facies records the broad lower sabkha just landward of the tidal flat. This interpretation is based on the features listed above, which have been well documented in the lower to middle zones of the modern Persian Gulf sabkha, and on a stratigraphic position above the Laminite Facies. The initial sediment was mainly lime mud transported from the subtidal to intertidal zones and subsequently dolomitized. At some locations, the sediment contained considerable amounts of clay. The anhedral mosaic fabric resembles Recent dolomite of the Gulf sabkha, which is associated with hypersaline pore waters (McKenzie et. al., 1980). Alternation of dolomite and dolomite-limestone layers in the Tonoloway may indicate widely fluctuating salinity levels in the sabkha pore waters.

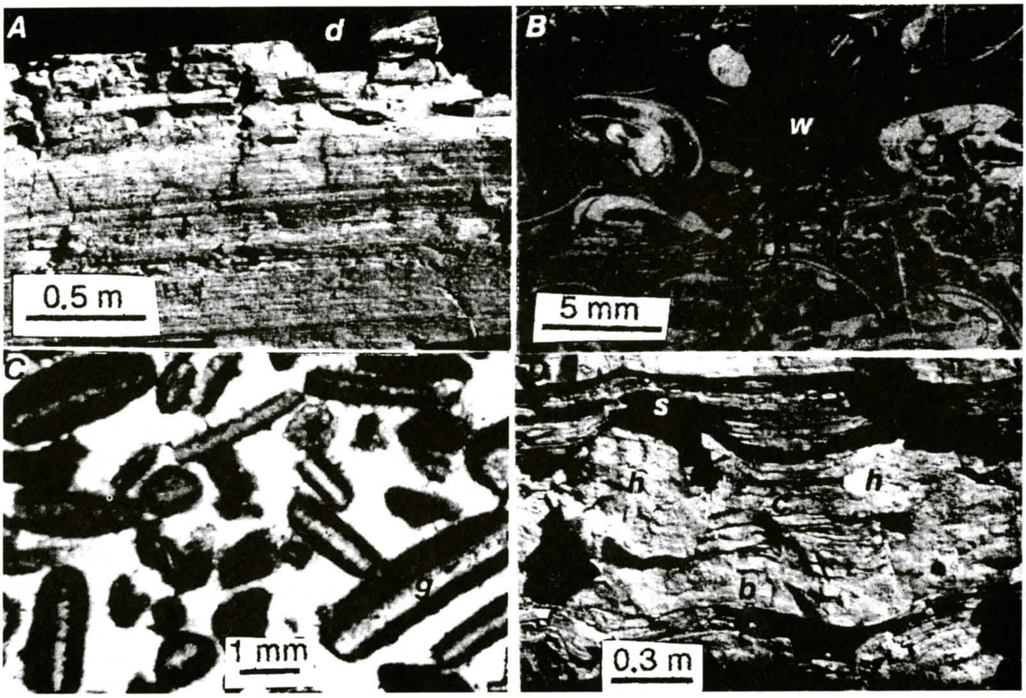

Figure 4. Examples from the Carbonate Lagoon-Sabkha Facies Association. A. Laminite Facies, with characteristic deep polygon dessication cracks (arrow shows example) (outcrop photo). Overlying Dolomite Facies (d) is mostly removed by weathering. B. Thin graded wackestone (w)/packstone (p) couplet (Peloidal/Oolitic Facies) (thin-section photo). Grains are mainly peloids (black) and thin ostracode shells. C. Peloidal/oolitic ostracode-rich grainstone (thin-section photo). Nuclei of elongate grains are ostracode shells (g shows example). Note that oolite coats have radial fabric. Calcite spar cement fills intergranular pores. D. Algal Facies: Outcrop photo showing example of a thrombolite biostrome (b) and biohermal heads (h) with connecting layers (c) and stromatolitic cap (s). This is part of a thrombolitic limestone interval present in the lower Tonoloway at some locations.

Bedded Mudstone Facies

This facies consists mainly of thin-bedded mudstone and wackestone, intercalated by algal limestone at many locations. Beds at the tops of sets are often very thin and appear to change imperceptibly upward into the Laminite Facies, which usually overlies them. Individual beds may be flat-laminated or massive, and the two types often alternate within sets. The main constituent is dense, pelleted lime mud, often with scattered microcrystalline dolomite, and variable amounts of whole and disarticulated ostracode shells. Other skeletal fragments may include brachiopods, gastropods, and bryzoans. There are also tiny, calcite-filled evaporite pseudomorphs, centimeter-scale halite molds, scattered masses of pyrite up to 1-2 mm diameter, and mudcracks. Very thin lags of ostracode debris and peloids in a partly argillaceous, dolomitic matrix frequently occur at the bottoms of beds and fill shallow scours. Burrows may be absent to abundant.

This facies records the inner part of the lagoon just seaward of the laminated intertidal flat. Daily energy conditions were low here. Texture, stratigraphic relationships, and paucity of dessication features support these interpretations. Low diversity, ostracode-dominated fauna and pelleted fabric suggest hypersaline, restricted lagoon conditions. Higher-diversity assemblages occurred under partly restricted to open conditions. The wackestone/ packstone layers are analogous to the storm layers described above in the Laminite Facies. The scours, thin lags, and intraclasts are also probably storm-related. Intercalated algal layers formed on the lagoon floor during periods of reduced sedimentation or perhaps during progradation. In the Persian Gulf, comparable pelleted sediments occur at depths of 5-15m (Purser and Evans, 1973). Pelleted mud also covers a wide area behind barrier shoals on the Bahama Platform just west of Andros Island in less than 4 m of water (Gebelein, 1974; Reading, 1996); this is the most protected part of the platform, with sediment being affected by waves and currents only during storms.

Peloidal/Oolitic Facies

This facies consists mainly of wackestone/ packstone to grainstone in which peloids and ostracodes, often oolitically-coated, constitute the predominant grain types (Figures 4B,C). The oolitic coatings have a radial fabric, vary in thickness from bed to bed or even among grains in the same bed, and are often superficial. Other grains may also include quartz sand/ silt, intraclasts, and aggregate grains. Skeletal material sometimes includes gastropods, brachiopods, echinoderms, bryzoans, and corals. Matrix is very similar to the bedded mudstone: micritic with a pelleted, partially dolomitized microfabric. The most important lithologies are graded wackestone/packstone (Figure 4B) and oolitic peloid/ostracode packstone/ grainstone (Figure 4C). The wackestone/packstone tends to occur above the packstone/grainstone in thin couplets which share specific characteristics with the tempestites described later, including erosional bedding contacts and shaly, dolomitic tops. The packstone/grainstone occurs in flat beds of medium thickness. Beds of well sorted ooid grainstone occur but are rare. Algal beds, lime mudstone/wackestone, and intraclast layers may be intercalated. This facies is usually overlain by the Bedded Mudstone Facies.

The Peloidal/Oolitic Facies was deposited in the outer parts of the subtidal lagoon laterally transitional with the nearshore lime mud flats of the previous facies. Circulation was generally restricted, but beds containing a higher-diversity fauna record more open-marine conditions. These interpretations are supported by the features and stratigraphic relationships described above. Farthest offshore was the packstone/ grainstone, behind which the wackestone/ packstone formed. We interpret that the energy level increased gradually seaward from the shoreline. Modern radial ooid fabrics suggest that maximum daily energy levels were only moderate and that hypersaline conditions existed (Loreau & Purser, 1973; Davies & Martin, 1976; Heller and others,1980; Reijers and ten Have, 1983), although radial fabrics associated with calcitic mineralogies appear to be predominant in Paleozoic ooids (Wilkinson and others, 1985). Close similarities between the graded wackestone/ packstone and tempestites indicate that higher energy levels in the lagoon resulted primarily from storm activity. Modern ooid deposits in the Persian Gulf (Loreau and Purser, 1973), Bahamas (Ball, 1967; Harris, 1979, Hine and others, 1981), and Shark Bay (Hagan and Logan, 1974) form in maximum water depths of 3-5 meters. Maximum possible depths for Tonoloway grainstones are constrained by wave base (perhaps 15 meters).

Intraclastic Facies

This facies consists of laterally continuous beds of limestone breccia or intraclast conglomerate. Such beds are relatively infrequent in the Tonoloway and occur locally as intercalations within or between other facies. Thin, laterally discontinuous layers are more common. Intraclast beds are more common than the breccias and contain oval, well rounded clasts which range from granule- to pebble-size and match the lithology of the underlying bed. Matrix can be composed of a varied mixture of allochemical grains and micrite. Notably, intraclasts often occur immediately above the Dolomite or Laminite Facies. The breccias occur within sets of bedded mudstones as beds which pinch and swell in outline and appear coarsely porous due to dissolution of matrix or selected clasts. The clasts are gravel- to coarse-sand-size, highly angular, and show a fitted ("jigsaw puzzle") arrangement. Some appear leached, contain spar-filled evaporite molds, and show a zonal weathering pattern of reddish-brown cores surrounded by paler rinds (Tourek,1970).

The laterally continuous beds of intraclast conglomerate above supratidal or intertidal beds most likely resulted from transgressional reworking of the underlying, partially lithified sediment. Discontinuous layers were probably generated during intermittent high-energy events (storms or tides). The breccia beds are interpreted as collapse breccias associated with evaporites and mudstone dissolution. Stratigraphic relationships and sedimentary features thus indicate an intertidal to supratidal range for this facies.

Algal Facies

This facies includes thrombolitic and stromatolitic limestones and interlayered or hybrid varieties of the two. Although clotted and massive algal fabrics have been classified as separate elsewhere (Aitken, 1967; Kennard and James,1986), the two are identified here as thrombolitic and differentiated from stromatolitic limestones by a lack of well-developed lamination. Thrombolitic limestone occurs in the Tonoloway mainly as biostromal beds centimeters or tens of centimeters thick containing domed or mounded forms. Various stromatolitic morphologies occur in individual, laterally continuous beds, as draping layers covering domed features (particularly thrombolite mounds), or as laterally discontinuous layers. The Algal Facies occurs mainly as intercalated beds within other carbonate-lagoon facies, particularly the Bedded Mudstone Facies. However, a single, distinct interval of stacked thrombolitic bioherms and biostromes totaling up to twelve meters in thickness occurs in the lower member at some locations (Figure 4D).

Intercalation of the various types of algal limestone with lagoon facies indicates that the different microbial organisms involved with their construction thrived on the lagoon floor when conditions were favorable and sometimes competed with each other for space. These algal beds probably record intervals of slow mechanical deposition (perhaps periods between storms) and/or hypersaline conditions which precluded fabric-disruptive grazing and boring fauna in the lagoon. Thrombolite bioherms directly overlain by tidal-flat laminites record depths approximately equal to the final synoptic relief of the bioherm above the sea floor (1 meter maximum).

Sandy Lagoon-Sabkha Facies Association

This association is volumetrically minor but environmentally important. It consists of two separate facies, each representing a quartz-rich variation of the lagoon, intertidal flat, and supratidal zone.

Mixed Carbonate-Siliciclastic Facies

This includes calcareous sandstone and dolomitic sandstone. The calcareous sandstone is represented by subequal amounts of very fine to fine quartz sand and pelleted micrite with variable amounts of clay and skeletal material. Some beds show bidirectional cross-stratification and partially preserved, asymmetrical and symmetrical ripple forms (Figure 5A). Planar beds with alternating, horizontal, quartz - dominated and micrite - dominated layers are also observed. Beds sometimes change upward into or consist of sandy, mudcracked laminites. Vertical burrows are locally present. Quartz grains are well sorted and angular to subrounded; some are highly rounded.

The calcareous sandstone bearing bidirectional cross-lamination, mudcracks, and horizontal lamination was deposited on a mixed carbonate-siliciclastic intertidal flat. The beds constructed of alternating quartz-rich and micrite-rich layers were deposited in the adjacent mixed carbonate-siliciclastic lagoon and may record either storm-segregated layering or pulses of quartz sand into the lagoon. The angular quartz grains and clay in these lithologies were washed in from landward areas, probably from the adjacent sabkha.

The dolomitic sandstone is identical to the Dolomitic Facies except for variable quantities of quartz sand and silt either disseminated throughout the dolomitic rock or concentrated in intercalated layers one to several centimeters thick. Quartz grains are moderately to well sorted, rounded to angular, and weather characteristically brown. Some beds weather shaly and

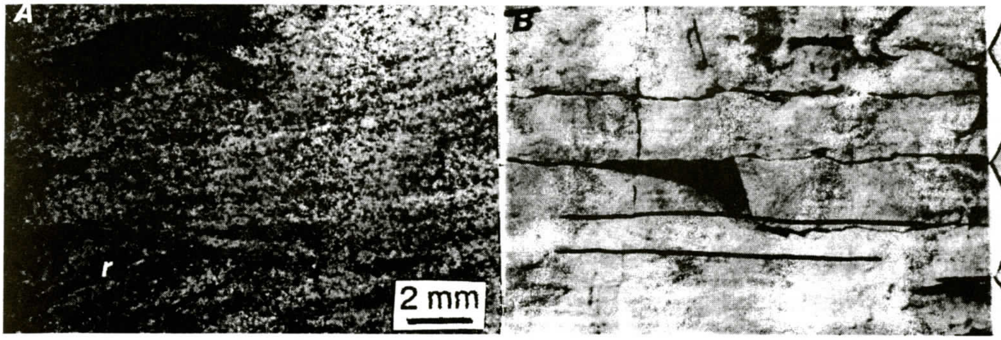

Figure 5. Examples from the Sandy Lagoon-Sabkha Facies Association. A. Mixed Calcareous-Siliciclastic Facies: Calcareous sandstone, cross-stratified variety (thin-section photo). Light-colored laminae are very fine, well-sorted quartz sand; dark areas are micrite and clay. Note preserved ripple form (r) (lower left) B.Siliciclastic Facies: Gray sandstone (outcrop; scale in dm). Light-colored layers (thicker example outlined) are very well-sorted quartz sand. The alternate, darker layers weather orange-brown and contain quartz sand and silt with variable amounts of clay and other material.

apparently contain a considerable amount of argillaceous material.

Like the Dolomite Facies, the dolomitic sandstone records a broad sabkha. The presence of quartz sand, however, suggests conditions more like those of the upper sabkha. The sand was most likely transported here both by water and wind from landward areas, as it was transported to the intertidal flat and lagoon where calcareous sandstone occurred.

Siliciclastic Facies (Indian Springs Sandstone)

This facies consists of intimately associated tabular units of gray sandstone, green muddy siltstone, and red siltstone. It is equivalent to the Indian Springs Sandstone Member of Swartz(1923), which is restricted to the east-central part of the basin around western Maryland. Outcrops tend to be scarce, small, and mostly covered.

The gray sandstone is highly indurated and occurs in thin horizontal beds amalgamated into sets up to 3 m thick (Figure 5B). Each bed weathers as a layer of fine- to medium-grained, massive quartz arenite overlain by a layer of very fine quartz sand and silt with a variable amount of clay matrix and some micrite. These couplets are texturally analogous to the graded thin wackestone/packstone of storm origin described in detail above under the Peloidal/Oolitic Facies. Quartz grains are angular to subrounded and very well sorted in the arenite layers, but the silty layers show bimodal sorting. Cross-laminated units occur infrequently. Sand-filled burrows are seen on some bedding planes.

The green siltstone occurs in medium to thick beds which appear shaly where deeply weathered. Quartz grains are mainly mud-supported, range from silt- to medium-sand-size, and are poorly sorted. The matrix of clay minerals and partly pelleted lime mud is compacted in places, forming dark wisps and swirls. These siltstones are frequently underlain by units of gray sandstone.

The red siltstone is maroon to light red, massive or vaguely layered, and may have a shaly layer and/ or mudcracks at the top. Evidence for channels appears to be absent, and there is no good evidence for wave or tidal-current activity. The fabric consists mainly of mud-supported quartz silt in a fine matrix which is colored dark red and assumed to be hematitic.

The gray sandstone was deposited in a shallow subtidal environment bordering the carbonate lagoon. This interpretation is supported by relatively high levels of sorting and maturity, incorporation within a carbonate unit, the presence of small amounts of carbonate material, burrows, and lack of dessication features. Comparison of the graded couplets to similar examples from ancient and modern records indicates that deposition was storm-dominated. Reineck and Singh (1972, 1980) described similar couplets deposited from suspended sand-mud mixtures during waning storms on subtidal flats at depths down to 10m in the German Bay area, North Sea. The green siltstones record a protected siliciclastic tidal flat shoreward of the gray sandstone. Levels of agitation were low, and reducing conditions possibly existed in the sediment pore water. Poor sorting and low maturity, stratigraphic association with the gray sandstone, and green color support these interpretations. These green beds frequently alternate with beds of red siltstone, and possible environmental analogues for the two together are discussed below.

Red color, mudcracks, association with the green siltstone and gray sandstone, and lack of channeling together suggest a low-energy marginal-marine environment which was subaerially exposed. The red siltstone was deposited on a siliciclastic supratidal flat transitional with alluvial-plain deposits landward. Rahmanian (1979) interpreted similar red beds associated with green silty beds in the Irish Valley Member of the Catskill Formation (Devonian) in Pennsylvania. A possible modern analogue for the associated red and green siltstones is the upper intertidal and supratidal zone in the northern Gulf of California near the mouth of the Colorado River where red, mudcracked silt and mud accumulate in extensive flats, and the entire tidal-flat complex is exposed to low wave energy and is relatively unchannelled (Thompson, 1968; Weimer and others, 1982).

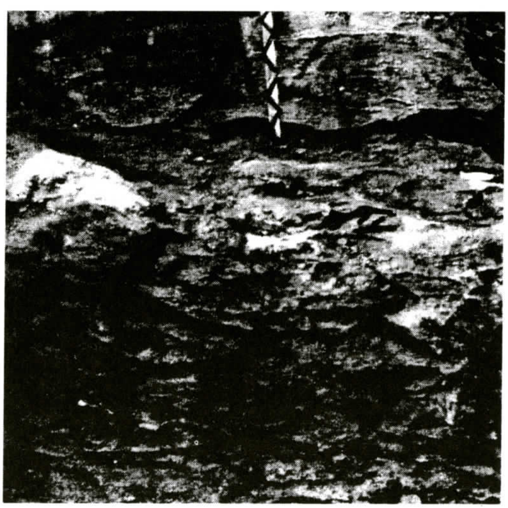

Figure 6. Crinoidal Grainstone Facies (Shallow Ramp Association) (outcrop photo). Lower two-thirds of photo shows very coarse-grained cross-stratified crinoidal grainstone with preserved wave- and ripple forms (examples of small ripples outlined near top). Bed in upper third of photo is slightly finer-grained and constructed of low-angle cross beds. Scale marks (top center) are dm.

Shallow Ramp Facies Association

This association represents a succession of high-energy shoal and offshoal environments.

Crinoidal Grainstone Facies

This facies consists of pelmatozoan-rich, cross-bedded skeletal grainstones in laterally continuous, resistant, tabular units up to 3.5 m thick (Figure 6). Many are coarse-grained, containing skeletal fragments measuring up to several centimeters or longer. The highly diverse fauna also includes bryzoans, brachiopods, ostracodes, and corals. Quartz sand is common. Cross-stratification includes large-scale tangential cross-beds and wedge-shaped packages of bidirectional laminae; smaller ripples are preserved near the tops of some units. Bedding planes, cross-stratification surfaces, and hardgrounds are sometimes encrusted by metazoans. Units of coarse grainstone may be superimposed on each other and separated by horizontal erosion surfaces. These surfaces may also be overlain by finer skeletal grainstone or rare oncoidal layers.

This facies records large shoals and banks of coarse skeletal material constructed by high wave and tidal energy, as indicated by coarse texture, high maturity, and cross-bedding. The shoals became mobilized and migrated laterally, probably during major storms, as indicated by the laterally continuous, tabular geometry of units. During periods of slower sedimentation, surfaces were partly stabilized by encrusting metazoans, and occasional hardgrounds formed as a result of sea-floor cementation and erosion. These shoals may have developed from crinoid thickets (c.f.Crowley, 1973). The diverse metazoan assemblage clearly demonstrates well oxygenated, well circulated, open-marine conditions. Analogous shoals have been documented at water depths of 5-20 m in Shark Bay (Hagan and Logan, 1974) and on the seaward edge of the Great Pearl Bank (Purser and Evans, 1973).

Mixed-Skeletal Facies

This facies is represented by skeletal floatstone or wackestone/packstone and framestone (Figures 7A, B). The lime mud matrix is dense and usually consists of pelleted micrite, sometimes with scattered, micron-scale dolomite rhombs, various amounts of clay, silt, or sand, and fossil hash. Less frequent matrix-poor varieties include cleaner stromatoporoid framestone (Figure 7A). Floatstone and wackestone/packstone beds are crinoid-rich and may contain vague/ highly disturbed/ partly-graded cross-laminations. These beds commonly grade downward into crinoidal grainstone and upward into nodular-bedded limestone. Stromatoporoidal limestone occurs as framestone or floatstone in massive, laterally continuous, tabular biostromal beds up to 2 m thick containing hemispherical and/or globular colonies. Bryzoan-rich limestone occurs as framestone, floatstone, or bafflestone; trepostomes appear to be the most frequent forms (Figure 7B). *In situ* corals include individual favositids from one to several centimeters; they occur mainly in floatstones and muddy framestones but rarely dominate the framework. This facies is usually associated with both the Crinoid Grainstone and Nodular Facies.

This facies records a transitional series of shoal-to-offshoal environments between fair-weather and storm wave-base (Figure 9.B), as indicated by the range of fabrics and stratigraphic position between high-energy shoal grainstones and the muddy Nodular Facies. Abundant, diverse fauna indicates well oxygenated, normal-marine conditions. Stromatoporoid biostromes and other clean skeletal framework developed under moderate- to high-energy conditions within wave base. Muddy framework and floatstone-wackestone/packstone developed in deeper, quieter water. A mud-tolerant fauna thrived here, but other skeletal fragments (particularly crinoids) were transported and deposited here periodically, presumably by storms. Storm-related activity may have also produced the graded, cross-laminated layers, which were subsequently disturbed by burrowing activity. Skeletal sediments similar to the Mixed-Skeletal Facies exist behind the Great Pearl Barrier in the Persian Gulf at depths ranging 5-15 m (Purser and Evans, 1973) and in Shark Bay at 10-30 m (Logan and Cebulski, 1970).

Nodular Facies

These limestones are identical in appearance to the nodular-bedded limestones in the Keyser Limestone immediately above the Tonoloway (see Head, 1969; Dorobek and Read, 1986). Beds have a characteristic lumpy appearance due to centimeter-scale nodules of fossil-peloidal wackestone-packstone surrounded by dark, clay-rich mudstone-wackestone (Figure 7C). This matrix contains peloidal micrite, clay, scattered microcrystalline dolomite, and ostracodes, with fewer brachiopods, gastropods, and pelmatozoans. Swarms of microstylolites locally extend into the edges of the nodules. Some thin zones of the dark mud oriented at steep angles to bedding resemble burrows. Either massive or shaly-weathering varieties of nodular limestone occur in tabular, laterally continuous sets up to several meters thick. Individual beds average 2-15 cm thick and often have poorly defined, wavy contacts. Shaly-weathering varieties resemble poorly-bedded mudstones containing widely separated packstone clusters. This facies occurs most often above and is gradational with the Mixed Skeletal Facies, particularly skeletal floatstone/ wackestone. It is also vertically gradational with graded thin wackestone/packstone or thin mudstone/ wackestone in the Carbonate Lagoon Facies at some locations.

Nodular bedding in limestone has been attributed to diagenetic processes, including early cementation of the nodules, compaction, and pressure solution (Shinn, 1977; Wanless,1979), along with some burrowing. This facies formed

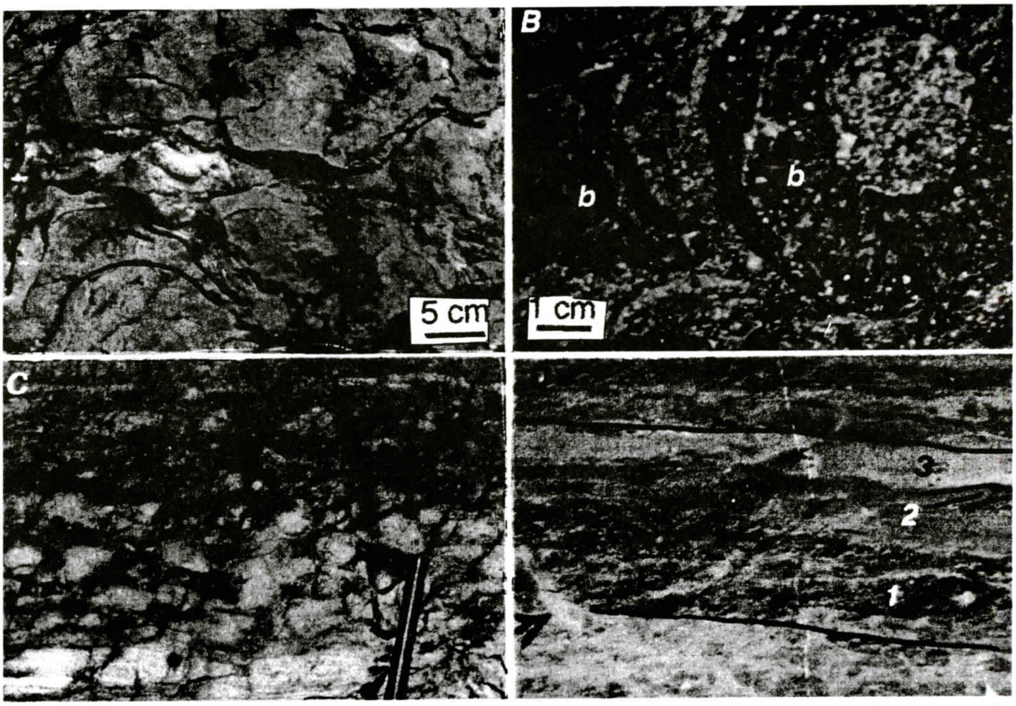

Figure 7. Example facies from the Shallow Ramp Association (A-C) and Deep Ramp (D). A and B: Mixed-Skeletal Facies: A. Massive stromatoporoid framestone (example colonies outlined at lower left) (outcrop photo). B. Skeletal floatstone/wackestone/packstone containing large trepostome bryzoans (b) (outcrop photo). Matrix is micrite with some clay. C. Nodular Limestone Facies (outcrop photo). Light-colored areas are nodular skeletal packstone. Enclosing matrix is compacted clay-rich wackestone. Skeletal material includes ostracodes and brachiopods. Pen is 8 cm. D. Tempestite Facies (Deep Ramp). Outcrop example of a triplet: 1-shelly packstone basal layer; fossils include crinoids and ostracodes; 2-rippled layer of silt-size carbonate (example of preserved ripple outlined at right); 3-clay-rich top layer. Arrow (lower left) indicates a burrow. Total thickness of unit is 25 cm.

between fair weather wave base and storm wave base on the muddy sea floor in deep areas between shoals, as indicated by muddy texture and stratigraphic association with the Mixed-Skeletal Facies. The original deposit apparently consisted of repetitive thin beds of lime mud and shell material, each grading at the top into a thin, clay-rich layer. Conditions varied from normal marine (for sediments with more diverse stenohaline fauna) to more restricted. Segregation of the clay-rich and shelly micritic layers was probably related to storm-reworking of the sediment. Nodular limestone associated with lagoonal facies probably formed at much shallower depths.

Deep Ramp Tempestite Facies

This facies consists of upward-fining limestone units several centimeters to several decimeters thick which repeat vertically in amalgamated sets up to 20 m thick. Units have erosional lower contacts and may occur as couplets or triplets (Figure 7D). In both, the lower part consists of massive or poorly laminated, shelly packstone/wackestone/floatstone, sometimes containing a thin layer of intraclastic lag at the bottom. Rare, preserved wave forms occur locally. Units are capped by laminated, silt- to mud-size carbonate which becomes more finely laminated, shaly, and dolomitic toward the top. Triplets contain a middle layer of well sorted, rippled, silt-size carbonate. Vertical or inclined burrows often penetrate one or even several subjacent units.

The units in this facies are tempestite deposits formed of shelly, muddy sediments below fair weather wave base in an open, storm-dominated environment. During storm peaks, the sediment was reworked into lags as wave base was lowered. Silty laminated layers, sometimes rippled, were deposited by waning-stage currents, followed by muddy layers which settled out from suspension and were burrowed between storms. This interpretation is based on comparison with similar packages documented elsewhere with a basal bioclastic packstone, fining-upward trend in texture, and sedimentary structures indicating storm reworking of the seafloor (cf. Kreisa, 1981; Kreisa and Bombach, 1982). According to those studies, reworking occurs between fairweather wave base (15 m) and storm-wave base (40 m). In the Tonoloway, this facies is followed upward by the Crinoidal Grainstone Facies, but individual beds or very thin intervals of tempestites were occasionally observed as intercalations within other subtidal carbonate facies. Deep ramp tempestite facies similarly overlain by crinoid shoal facies were described in Lower Mississippian carbonates of Wyoming and Montana by Elrick and Read (1991).

REGIONAL FACIES-ENVIRONMENT MODEL

Four regional-scale facies and depositional environments correspond to the four facies associations outlined in the previous section. These are correlated across the study area in Figure 10 and summarized briefly below. Correlations show that the three principal types of environments - lagoon-sabkha, shallow ramp, and deep ramp - all coexisted to form an array along the length of the study area during the time represented by the middle Tonoloway (see Figures 10 and 11A). Based on this array, on vertical transitions among the included facies (Figure 8), and on the characteristics of the subenvironments represented, we have constructed a comprehensive facies model for the Tonoloway Limestone (Figure 9, top) which shows a

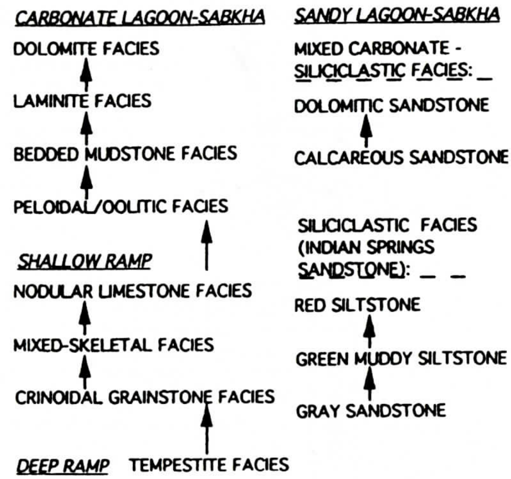

Figure 8. Idealized vertical transitions among Tonoloway facies and facies associations, based on stratigraphic relationships observed in outcrop sections. Carbonate facies appear in the left column, sandy facies in the right.

transition from a carbonate lagoon-sabkha on the northeast to a shallow ramp and deep ramp on the southwest. The upward-shallowing trends among facies shown in Figure 8 are assumed to be the result of shoreline progradation and lateral facies migration related to sea-level changes.

Carbonate Lagoon-Sabkha

This is represented by the Carbonate Lagoon-Sabkha Facies Association and consists of a shallow carbonate lagoon, adjacent intertidal flat, and supratidal sabkha (see Figure 9A).

Oolitic-peloidal-skeletal sands and lime mud in the lagoon passed transitionally landward into laminated lime mud on the intertidal flat and then into arid, dolomitic sabkha sediments. These subenvironments occurred on an epeiric platform which sloped quite gently seaward toward the southwest. This is the dominant regional facies. It constitutes the entire upper member and all but the very top of the lower member; in these parts of the Tonoloway, the lagoon was restricted. In parts of the middle member, where this facies is confined to the northeastern part of the study area, the lagoon was partly restricted or open.

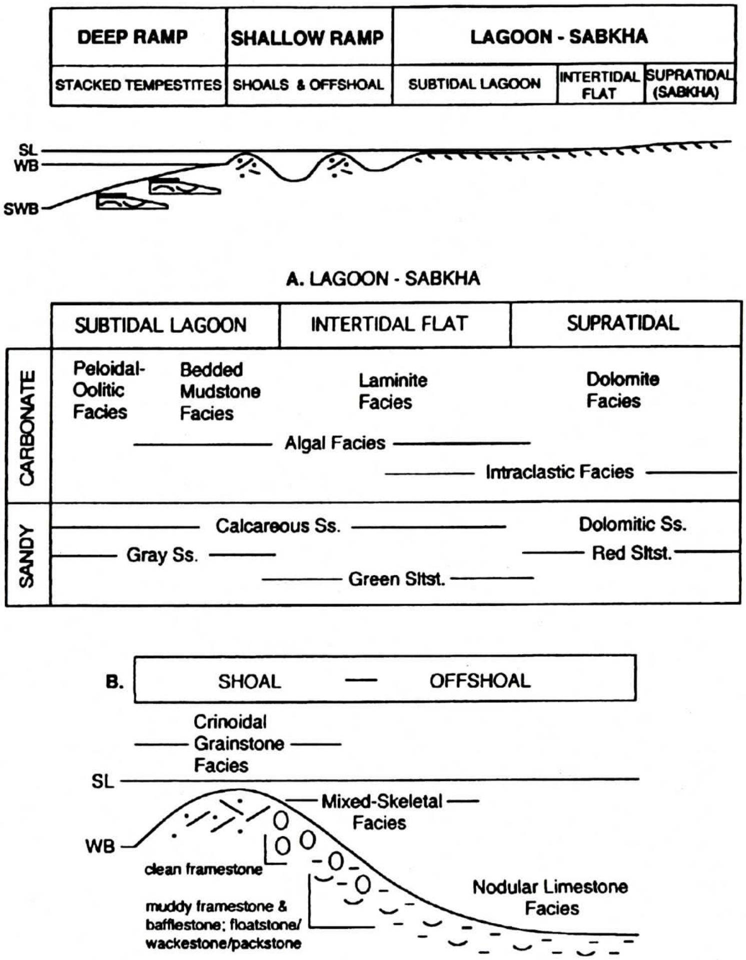

Figure 9. Tonoloway facies-environment models: Comprehensive regional model (top) shows principal environments and subenvironments arrayed in profile. This complete array is recorded from northeast (right) to southwest (left) in the middle Tonoloway (see Figure 11A and time A on the Regional Facies Diagram). A. shows lateral distributions of facies in the Carbonate- v.s. Sandy versions of the Lagoon-Sabkha. B. shows the continuum of facies between adjacent shoal-offshoal environments of the Shallow Ramp. Important lithologies in the Mixed-Skeletal Facies are in small print. Diagrams are purely schematic and based on all information in this study concerning Tonoloway facies and their relationships. SL- sea level; WB- wave base (15 m, assumed); SWB - storm wave base (40 m, assumed).

Sandy Lagoon-Sabkha (Figures 9Aand 11B)

This is represented by the Sandy Facies Association, which consists of Mixed Carbonate-Siliciclastic Facies and Siliciclastic Facies. The Mixed Facies represents the same transitional lagoon, intertidal flat, and sabkha as the carbonate lagoon-sabkha, but quartz sand and silt were mixed or interlayered with the carbonate sediments. In the Siliciclastic Facies (Indian Springs Sandstone Member), confined to a local lobe area along the eastern side of the mixed lagoon, subtidal quartz silt and sand passed shoreward into intertidal flats of green mud and then into marginal-marine flats of red silt. The Sandy Lagoon-Sabkha is stratigraphically confined to a thin interval the very top of the lower Tonoloway.

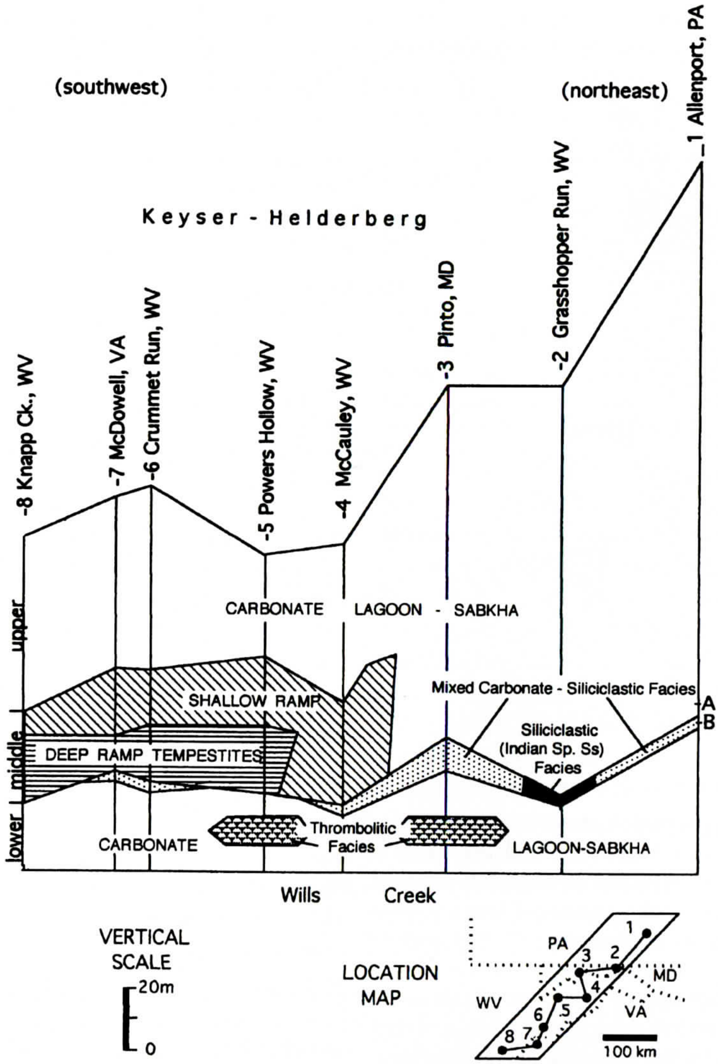

Figure 10. Regional facies correlation diagram for the Tonoloway Limestone. Major facies associations (Carbonate Lagoon-Sabkha, Sandy Lagoon-Sabkha, Shallow Ramp, and Deep Ramp-Tempestites) are shown correlated among the eight principal outcrop sections from the Study Area Map. Datum is the lower boundary of the Tonoloway with the Wills Creek Formation. The Mixed- and Siliciclastic Facies of the Sandy Association and local thrombolitic versions of the Carbonate Lagoon-Sabkha Facies are shown individually. Tonoloway stratigraphic members are indicated on left side. Time lines are assumed parallel to facies boundaries; A - point on a time line extending southwest through the Carbonate Lagoon-Sabkha, Shallow Ramp, and Deep Ramp Facies; B - point on a time line extending southwest through Sandy Lagoon-Sabkha Facies. Paleogeographic maps corresponding to times A and B are shown in Figure 11.

Shallow Ramp (Figure 9B)

This is represented by the Shallow Ramp Facies Association and consisted of large-scale skeletal shoals separated by deeper, more protected offshoal areas in an open environment. With increasing depth, cross-bedded crinoid grainstone above wave base on the shoals passed into an offshoal/intershoal succession of skeletal limestones, and, above storm wave

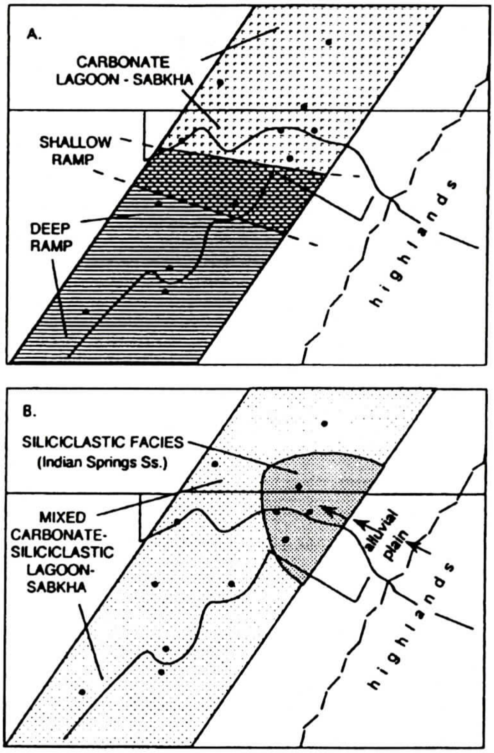

Figure 11. Paleogeographic maps of the study area showing facies-environments during middle Tonoloway time (11A) when the complete array of major carbonate environments (Figure 9, top) extended northeast-southwest across the region, and during the latest part of lower Tonoloway time (11B), when sandy facies predominated regionally. 11A and B correspond to times A and B, respectively, on the Regional Facies Diagram. The lobate area of Indian Springs Sandstone is shown transitional with an alluvial plain landward in 11B; arrows indicate assumed major direction of drainage to this part of the coast. Data points correspond to outcrop locations shown on the Study Area Map. Vertical and horizontal scales are slightly distorted due to figure resizing; actual study area dimensions are approximately 100km E-W and 330km NE-SW.

base in the deepest areas, nodular limestone. The Shallow Ramp was located between the Deep Ramp and Lagoon-Sabkha and is restricted stratigraphically to the middle Tonoloway in the southern part of the study area (see Figures 10 and 11A).

Deep Ramp

This was an open, storm-dominated environment in which lime mud and skeletal material were reworked and deposited near storm wave base in graded units. As with the Shallow Ramp, the Deep Ramp was also restricted to the middle member in the southern part of the study area.

DISCUSSION: RAMP DEVELOPMENT

The carbonate ramp in this study is of particular interest, because this depositional setting has not been previously recognized in the Tonoloway Limestone or other pre-Helderberg units in the thick Siluro-Devonian carbonate succession of the central Appalachian basin. Possible controls on the ramp's development by sea-level and tectonic mechanisms are discussed in this section.

The sharp transition from shallow, restricted lagoon conditions in the lower Tonoloway to deeper, open marine conditions clearly indicates that a transgression accompanied ramp development in the middle member throughout the southern part of the study area (see Figure 10). Partly-restricted or open conditions in some parts of the lagoon to the northeast provides evidence of the transgression on the northern part of the platform. A region-wide return to shallow, restricted conditions, recorded by the upper Tonoloway, indicates that ramp development later ceased and the area once again became an epeiric platform, remaining so throughout the latter part of Tonoloway time. The Tonoloway-Helderberg contact records the onset of the next transgression above the Tonoloway (Head, 1969; Dorobek and Read, 1986; Dorobek, 1992). This supports an overall regressive-transgressive-regressive sea-level pattern for the Tonoloway, with ramp development coinciding with the transgression.

Based on that, it first appears that ramp development in this case might be explained simply by transgressive deepening along the platform slope. However, contrasts in water depth, bathymetric slope changes, and sharply aggradational facies relationships strongly indi-

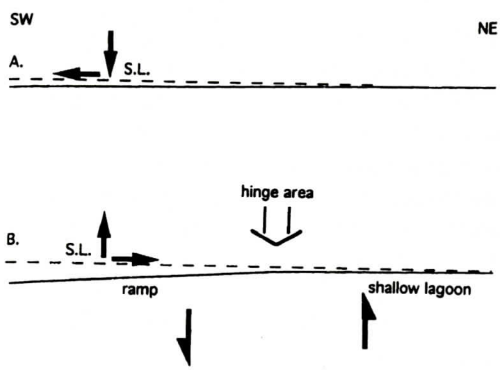

Figure 12. Schematic profiles of the study area illustrating bathymetric and sea-level changes discussed in the text. 12A represents the profile throughout upper and lower Tonoloway times, when the entire seaway consisted of a shallow epeiric platform, and long-term sea-levels were falling. 12B represents the profile during ramp development in middle Tonoloway time. It shows significantly steeper slopes developed on the southeastern part of the platform adjacent to the remainder of the shallow lagoon on the northeast and rising long-term sea-levels related to a northeastward transgression. Ramp facies developed on the south side of the slope "hinge" in response to the resulting increase in water depths. Opposing directions of relative vertical tectonic displacements on either side of the "hinge" that would produce this bathymetric slope change are shown by the vertical arrow pair beneath the profile. Details are discussed in the text.

cate the possibility that local or regional tectonic mechanisms were involved (see Figures 9(top), 10, and 11A). Figure 12 illustrates the changes in Tonoloway sea level and bathymetry discussed here. Even casual inspection of the contrast in maximum water depths between the ramp and the lagoon-sabkha (i.e. 40m vs.15m, respectively) suggests that the southwestern area subsided much more rapidly at some point. This difference in depth (i.e. 40m -15m = 25m) divided by the minimum horizontal distance between the lagoon-sabkha and deep ramp (i.e. the width the shallow ramp: approximately 45km) yields an estimate of 0.0006 for maximum possible slopes on the ramp. Using the maximum horizontal distance along the ramp within the study area (approximately 196km) yields a estimate of 0.0001 for minimum slopes on the ramp. The average of these two extremes, 0.0004, is still twice the maximum for epeiric platform slopes (0.0002)(Irwin, 1965), and it closely approximates the overall slope of the modern Persian Gulf ramp (0.0005). Finally, regional relationships among the deep ramp, shallow ramp, and lagoon-sabkha facies were sharply aggradational (versus the progressively onlapping retrogradational style predicted by transgression along a constant slope) throughout the time the three coexisted (see Figure 10).

This set of observations indicates that slopes on the part of the platform destined to become the ramp had already increased significantly by the time transgression began, and this cannot be explained by the simple hypothesis of deepening along a uniform platform slope. It is best explained by relative downward tectonic displacement on the south side of a "hinge" (Figure 12B). The resulting difference in slope between the two parts of platform on either side of the "hinge" would account for the observed contrast in water depths, with ramp facies developing in response to deepening on the south side. Overall rising sea-level above this hinged bathymetric profile would then produce the observed aggradational facies relationships, assuming that rates of accommodation space-filling were uniform across the study area.

A widely accepted tectonic mechanism for transforming carbonate platforms into ramps is vertical fault displacement, as modeled by Wilson (1975). Studies by Donaldson and Shumaker (1981), Yeilding and Dennison (1986) and Linn and others (1990) cited evidence for basement normal-fault zones and invoked fault reactivation to explain anomalous facies patterns in Middle and Late Paleozoic units in the same general area of the Appalachian basin shown for the ramp in the present study (see Figure 11A). The locations and trends (east-west to northwest - southeast) shown for most of those structure zones match or nearly match the location and trend of the proposed Tonoloway "hinge" area, which coincides approximately with the area of the shallow ramp shown in Figure 11A. Linn and others (1990) documented fault-controlled carbonate facies in the Helderberg Group along a downdropped area whose northern boundary approximately coincides with the location of the Tonoloway "hinge". Furthermore, the proposed structural control on facies in that study and in the present study resulted in facies trends oriented northwest-southeast perpendicular to the basin axis. Dorobek and Read (1986) show deep ramp and deeper basin facies developed at various stages during Helderberg time in the same general map area shown for the ramp in the present study. These observations suggest that repeated vertical tectonic movement in that same general area of the Appalachian basin controlled anomalous facies development there at various times during the Paleozoic. Therefore, considering all the information presented, it is concluded that both transgressive sea-level activity and vertical tectonic displacement, probably fault-induced, acted as controls on the development of the Tonoloway ramp. The complete basin evolution of the Tonoloway Limestone and related sea-level fluctuations will be outlined in detail via a sequence stratigraphic analysis, currently in preparation by the authors.

SUMMARY AND CONCLUSIONS

We have identified, correlated, and established vertical relationships among four regional facies associations and their component lithofacies in the Tonoloway Limestone. From these, we have established regional-scale depositional environments and a comprehensive facies-environment model. The four lithofacies associations and corresponding environments are: Carbonate Lagoon-Sabkha, Sandy Lagoon-Sabkha, Shallow Ramp, and Deep Ramp-Tempestites. Ramp facies have not been previously recognized in the Tonoloway Limestone or other pre-Helderberg units in the Siluro-Devonian carbonate interval of the central Appalachian basin.

1) In the carbonate lagoon, moderate- to low-energy, oolitic sand (Peloidal/Oolitic Facies) offshore passed transitionally into nearshore mud flats (Bedded Mudstone Facies), mud-cracked intertidal flats (Laminite Facies), and sabkha (Dolomite Facies). Conditions varied from restricted to relatively open, depths were shallow (above wave base), and energy was storm-dominated.

2) Sandy Lagoon-Sabkha Facies are volumetrically minor. In the Mixed Facies lagoon, calcareous sand passed into cross-laminated calcareous sand and sandy laminite on the intertidal flat and sandy dolomite on the sabkha. In the Siliciclastic Facies lagoon, storm- graded gray quartz sand and silt passed into green muddy silt on the intertidal flat and red silt on an arid supratidal marginal-marine flat. Conditions and water depths were similar to those of the restricted carbonate lagoon-sabkha. The Siliciclastic Facies (Indian Springs Sandstone Member) was deposited near a major point of fluvial discharge along the eastern shoreline of the Mixed Facies lagoon.

3) The Shallow Ramp consisted of large-scale, high-energy skeletal grainstone shoals (Crinoidal Grainstone Facies) and offshoal areas (Mixed Skeletal Facies). Shoals and clean stromatoporoid biostromes formed within wave base (assumed to be 15 m) and passed into muddy framestone, bafflestone, and floatstone/wackestone/packstone with increasing depth offshoal. Frame builders included stromatoporoids, bryzoans, and corals. Burrowed, clay-rich skeletal packstone/wackestone (Nodular Limestone Facies) covered the surrounding sea floor. Maximum depth was between normal wave base and storm wave base (assumed to be 40 m). On the Deep Ramp, thin, graded storm units (Tempestite Facies) were deposited at or above storm wave base and consisted of shelly packstone bases overlain by silt- and mud-size carbonate with clay-rich layers at the top. Well circulated, open-marine conditions prevailed on both parts of the ramp.

4) The comprehensive Tonoloway model is a transitional array from a Carbonate Lagoon-Sabkha to a Shallow Ramp and Deep Ramp. This complete array was present during the middle part of Tonoloway time, when the southern part of the study area developed into the ramp. During the earlier and later parts of Tonoloway time, the seaway consisted of a regional epeiric platform bearing only lagoon-sabkha facies. The ramp developed from this

platform coincident with a northeastward regional transgression between two regressions, all within the 1-3 Ma span of Tonoloway time. Both transgressive sea-level activity and tectonic displacement acted as controls on ramp development; the latter was possibly due to basement-fault reactivation.

REFERENCES CITED

Aitken, J. D., 1967, Classification and environmental significance of cryptalgal limestones and dolomites, with illustrations from the Cambrian and Ordovician of southwestern Alberta: Journal of Sedimentary Petrolology, v. 37, p. 1163-1178.

Ball, M. M., 1967, Carbonate sand bodies of Florida and the Bahamas: Journal of Sedimentary Petrology, v. 37, p. 556-591.

Berry, W.B.N., and Boucot, A.J., 1970, Correlation of the North American Silurian rocks: Geological Society of America Special Paper 102, 289 pp.

Crowley, D.J., 1973, Middle Silurian patch reefs in Gasport Member (Lockport Formation), New York: American Association of Petroleum Geologists Bulletin, v. 57, p. 283-300.

Davies, P. J., and Martin, K., 1976, Radial aragonite ooids, Lizard Island, Great Barrier Reef: Geology, v. 4, p. 120-122.

Dennison, J.M., 1970, Silurian stratigraphy and sedimentary tectonics of southern West Virginia and adjacent Virginia, *in* Robertson, J.L., and Pertusio, S.M., eds., Silurian stratigraphy central Appalachian basin: Charleston, West Va: Appalachian Geological Society guidebook for field conference, April 17-18, 1970, Roanoke, Virginia, p. 2-23.

Dorobek, S.L., and Read, J.F., 1986, Sedimentology and basin evolution of the Siluro-Devonian Helderberg Group, central Appalachians: Journal of Sedimentary Petrology, v.56, p. 601-613.

Dorobek, S.L., 1992, Sequence development in the Siluro-Devonian Helderberg Gp., Cent. Appalachians, in Dennison, J.M. and others, Field Trip Guide No. 7: E. Sec. SEPM, p. 107-112.

Donaldson, A.C. and Shumaker, R.C., 1981, Late Paleozoic molasse of Central Appalachians, in Miall, A.D., ed., Sedimentation and Tectonics in Alluvial Basins: Geological Association of Canada Spec. Paper. 23, p.99-124.

Elrick, M., and Read, J.F., 1991, Cyclic ramp-to-basin carbonate deposits, Lower Mississippian, Wyoming and Montana: a combined field and computer modeling study: Journal of Sedimentary Petrology, v. 61, p. 1194-1224.

Gebelein, C. D., 1974, Guidebook for Modern Bahamian Platform Environments: Geological Society of America annual meeting Fieldtrip Guide, 93 pp.

Hagan, G.M., & Logan, B.W.,1974, Development of carbonate banks and hypersaline basins, Shark Bay, Western Australia, *in* Evolution and Diagenesis of Quaternary Carbonate Sequences, Shark Bay, Western Australia: American Association of Petroleum Geologists Memoir 22, p. 61-139.

Harland, W.B., Armstrong, R.L., Cox, A.V., Craig, L.E., Smith, A.G., and Walters, R., 1982, A Geological Time Scale: Cambridge Earth Science Series, Cambridge University Press, Cambridge, 246 pp.

Harris, P. M., 1979, Facies anatomy and diagenesis of a Bahamian ooid shoal, *in* Ginsburg, R. N., ed., Sedimenta VII: The Comparative Sedimentology Lab, Miami, Florida, 164 p.

Head, J.W., 1969, An integrated model of carbonate depositional basin evolution: Late Cayugan (Upper Silurian) and Helderbergian (Lower Devonian) of the central Appalachians: Unpublished Ph.D. dissertation, Brown University, Providence, R.I., 390 pp.

Helfritch, C.T., 1975, Silurian conodonts from the Wills Mountain Anticline, Virginia, West Virginia, and Maryland: Geological Society of America Special Paper 161, 82 pp.

Heller, P. L., Komar, P. D., and Pevear, D. R., 1980, Transport processes in ooid genesis: Journal of Sedimentary Petrology, v. 50, p. 948-952.

Hine, A. C., Wilber, R. J., and Neumann, A. C., 1981, Carbonate sand-bodies along contrasting shallow-bank margins facing open seaways, northern Bahamas: American Association of Petroleum Geologists Bulletin, v. 65, p. 261-290.

Irwin, M.L., 1965, General theory of epeiric clear water sedimentation: American Association of Petroleum Geologists Bulletin, v. 49, p. 445-459.

Kennard, J. M., and James, N. P, 1986, Thrombolites and stromatolites: two distinct types of microbial structures: Palaios, v. 1, p. 492-503.

Kinsman, D. J. J., 1964, The recent carbonate sediments near Halat el Bahrani, Trucial Coast, Persian Gulf, *in* Deltaic and shallow marine deposits: Developments in sedimentology, v. 1: Elsevier, Amsterdam, p. 189-192.

Kreisa, R. D., 1981, Storm-generated sedimentary structures in subtidal marine facies with examples from the Middle and Upper Ordovician of southwestern Virginia: Journal of Sedimentary Petrology, v. 51, p. 823-848.

Kreisa, R. D., and Bombach, R. K., 1982, The role of storm processes in generating shell beds in Paleozoic shelf environments, *in* Einsele, G., and Seilacher, A., eds., Cyclic and event stratification: Springer-Verlag, Berlin, p.200-207.

Linn, F.M., Textoris, D.A., and Dennison, J.M., 1990, Syndepositional tectonic influence on lithofacies of the Helderberg Gp. (Sil.-Dev.) of the Cent. Appalachians: in Shumaker, R.C., ed., Appalachian Basin Industrial Associates Fall Program, Morgantown, WV., v.17, p.190-211.

Logan, B.W., and Cebulski, D.E., 1970, Sedimentary environments of Shark Bay, western Australia, *in* Logan, B.W. and others, eds., Carbonate sedimentation and environments, Shark Bay, western Australia: Association of American Petroleum Geologists Memoir 13, p.1-37.

Loreau, J. P., and Purser, B. H.,1973, Distribution and ultrastructure of Holocene ooids in the Persian Gulf: *in* Purser, B.H., ed., The Persian Gulf: Springer-Verlag, Berlin, p. 279- 328.

McKenzie, J.A., Hsü, K.J., and Schneider, J.F., 1980, Movement of subsurface water under the sabkha, Abu Dhabi, UAE, and its relation to evaporative dolomite genesis, *in* Zenger, D.H., Dunham, J.B., and Ethington, R.L., eds., Concepts and models of dolomitization: Society of Economic Paleontologists and Mineralogists Special Publication 28, p. 11-30.

McKerrow, W.S., Lambert, R. St. J., and Cocks, L.R.M., 1985, The Ordovician, Silurian, and Devonian Periods, *in* Snelling, N. J., ed., The chronology of the geological record: Geological Society of London Memoir 10, p. 73-80.

Osleger, D., and Read, J.F., 1991, Relation of eustacy to stacking patterns of meter-scale carbonate cycles, Late Cambrian, U.S.A: Journal of Sedimentary Petrology, v. 61, p. 1225-1252.

Palmer, A.R., compiler, 1983, The decade of North American Geology 1983 geologic time scale: Geology, v. 11, p. 503-504.

Patchen, D.G., Avary, K.L., and Erwin, R.B, 1984, Correlation of stratigraphic units in North America (COSUNA) northern Appalachian region correlation chart: American Association of Petroleum Geologists Correlation Chart Series, Tulsa, Oklahoma.

Purser, B. H., and Evans, G.,1973, Regional sedimentation along the Trucial Coast, SE Persian Gulf, *in* Purser, B. H., ed., The Persian Gulf: Springer-Verlag, Berlin, p. 211-231.

Rahmanian, V. D. K., 1979, Stratigraphy and sedimentology of the Upper Devonian Catskill and uppermost Trimmers Rock Formations: Unpublished Ph.D. dissertation, Pennsylvania State University.

Reading, H.G., ed., 1996, Sedimentary environments, processes, facies, stratigraphy, 3rd ed: Blackwell Scientific, Oxford, 704 pp.

Reijers, T.J.A., and ten Have, A.H.M., 1983, Ooid zonation as indication for environmental conditions in a Givetian-Frasnian carbonate shelf-slope transition, *in* Peryt, T. M., ed., Coated grains: Springer-Verlag, Berlin, p. 188-198.

Reineck, H.E., and Singh, I.B., 1972, Genesis of laminated sand and graded rhythmites in storm-sand layers of shelf mud: Sedimentology, v. 18, p. 123-128.

Reineck, H.E., and Singh, I.B., 1980, Depositional sedimentary environments (second edition): Springer-Verlag, Berlin, 504 pp.

Salvador, A., 1985, Chronostratigraphic and geochronometric scales used in COSUNA stratigraphic nomenclature charts of the United States: American Association of Petroleum Geologists Bulletin, v. 69, p. 181-189.

Shinn, E. A., Halley, R. B., Hudson, J. H., and Lidz, B. H., 1977, Limestone compaction: an enigma: Geology, v. 5, p. 21-24.

Smosna, R.A., Patchen, D.G., Warschauer, S.M., and Perry, W.J.Jr., 1977, Relationships between depositional environments, Tonoloway Limestone, and distribution of evaporites in the Salina Formation, West Virginia, *in* Fisher, J.H., ed., Reefs and evaporites, concepts and depositional models: American Association of Petroleum Geologists Studies in Geology 5, v.49, p. 125-143.

Smosna, R.A., and Warschauer, S.M., 1979, A scheme for multivariate analysis in carbonate petrology with an example from the Silurian Tonoloway Limestone: Journal of Sedimentary Petrology, v. 49, p. 257-272.

Smosna, R.A., and Warschauer, S.M., 1981, Rank exposure index on a Silurian carbonate tidal flat: Sedimentology, v. 28, p. 723-731.

Swartz, C.K., 1923, Silurian Volume: Maryland Geological Survey, Baltimore, Maryland, 779 pp.

Thompson, R.W., 1968, Tidal flat sedimentation on the Colorado River delta, northwest Gulf of California: Geological Society of America Memoir 107, 133 pp.

Tourek, T.J., 1970, The depositional environments and sediment accumulation models for the Upper Silurian Wills Creek Shale and Tonoloway Limestone, central Appalachians: Unpublished Ph.D. dissertation, Johns Hopkins University, Baltimore, Maryland, 271 pp.

Wanless, H. R., 1979, Limestone response to stress: pressure solution and dolomitization: Journal of Sedimentary Petrology, v. 49, p. 437-462.

Weimer, R.J., Howard, J. D., and Lindsay, D.R., 1982, Tidal flats and associated tidal channels, *in* Scholle, P.A., and Spearing, D., eds., Sandstone depositional environments: American Association of Petroleum Geologists Memoir 31, p. 191-245.

Wilkinson, B.H., Owen, R.M., and Carroll, A.R., 1985, Submarine hydrothermal weathering, global eustacy, and carbonate polymorphism in Phanerozoic marine oolites: Journal of Sedimentary Petrology, v. 55, p. 171-183.

Wilson, J.L., 1975, Carbonate Facies in Geologic History: Springer-Verlag, Berlin, 471p.

Woodward, H.P., 1941, Silurian System of West Virginia: West Virginia Geological Survey, Volume XIV, 326 pp.

Yeilding, C.A. and Dennison, J.M., 1986, Sedimentary response to Mississippian tectonic activity at east end of the 39th Parallel fracture zone: Geology, v. 14, p. 621-624.

SOUTHEASTERN GEOLOGY
V. 38, No. 4, August 1999, p.279-290

LATE PLEISTOCENE THROUGH HOLOCENE DEGRADATIONAL SEQUENCE IN THE CHATTAHOOCHEE ALLUVIAL VALLEY BELOW THE FALL LINE

DONALD M. THIEME

Department of Geology
University of Georgia
Athens, GA 30601

ABSTRACT

Recent field investigations at Fort Benning, Georgia suggest that the Chattahoochee River was actively downcutting and migrating to the west between 47 and eight thousand years before present. As the river downcut, it filled its valley with coarse cross-bedded sand and gravel. The Laundry Creek Formation is introduced as a formal lithostratigraphic designation for the deposits from this degradational sequence. Similar sequences dated to the late Pleistocene and early Holocene are found in other alluvial valleys in the Southeast. Possible causes for this regional pattern of alluvial valley degradation are reviewed and tentatively evaluated.

INTRODUCTION

This report describes the geology and geomorphology of a degradational alluvial sequence in the Chattahoochee valley south of the Fall Line and provides regional correlates and possible mechanisms for a regional pattern of alluvial valley degradation. The Chattahoochee River is the principal drainage to the Gulf of Mexico from the Georgia Piedmont. Late Pleistocene through Holocene stratigraphic exposures in the alluvial valley were studied at Fort Benning in conjunction with an archaeological survey of Lawson Field (Figure 1). The study area is approximately 30 kilometers (km) downstream of Columbus, Georgia.

At Fort Benning, the Chattahoochee valley is incised approximately 10 meters (m) into Cretaceous lithologies. Radiocarbon dates obtained on samples collected from stratigraphic exposures described in this paper (see Table 1) constrain the timing of the incision. Between 47 and eight thousand years (ka) before present (B.P.) the river was actively downcutting and migrating to the west as it deposited coarse cross-bedded sand and gravel which now fill much of the alluvial valley. Finer textured overbank flood deposits are locally inset against the eroding scarp of the terrace constructed during valley degradation. Aeolian reworking has also redistributed some of the fines and sculpted the contours on Lawson Field.

Similar degradational sequences dating to the late Pleistocene and early Holocene are found in most alluvial valleys in the Southeast, particularly at and immediately downstream of the Fall Line. Surfaces constructed during valley degradation in Alabama (Maxwell, 1971; Szabo, 1973), the Mississippi alluvial valley (Saucier, 1994, p. 240-242; Autin and others, 1991), and Texas (Blum and others, 1995a, 1995b) are traditionally referred to as "Deweyville" terraces. While alluvial valleys in Georgia are as yet poorly studied, the sequences in the Ocmulgee (Cosner, 1973), Oconee (Brook, 1981), Ogeechee (Leigh and Feeney, 1995), and Savannah (Nystrom and Denham, 1999; Leeth and Nagle, 1996; Segovia, 1985) River valleys appear to resemble that described in this report for the Chattahoochee. Recent studies point to regional climate rather than sea level change as the mechanism causing incision (Leigh and Feeney, 1995; Saucier, 1981). Tectonism is a less frequently invoked mechanism which seems to have played a role within the present study area.

GEOLOGY AND GEOMORPHOLOGY OF THE DEGRADATIONAL SEQUENCE

The Lawson Field study area is in the Upper Coastal Plain approximately 30 km downstream

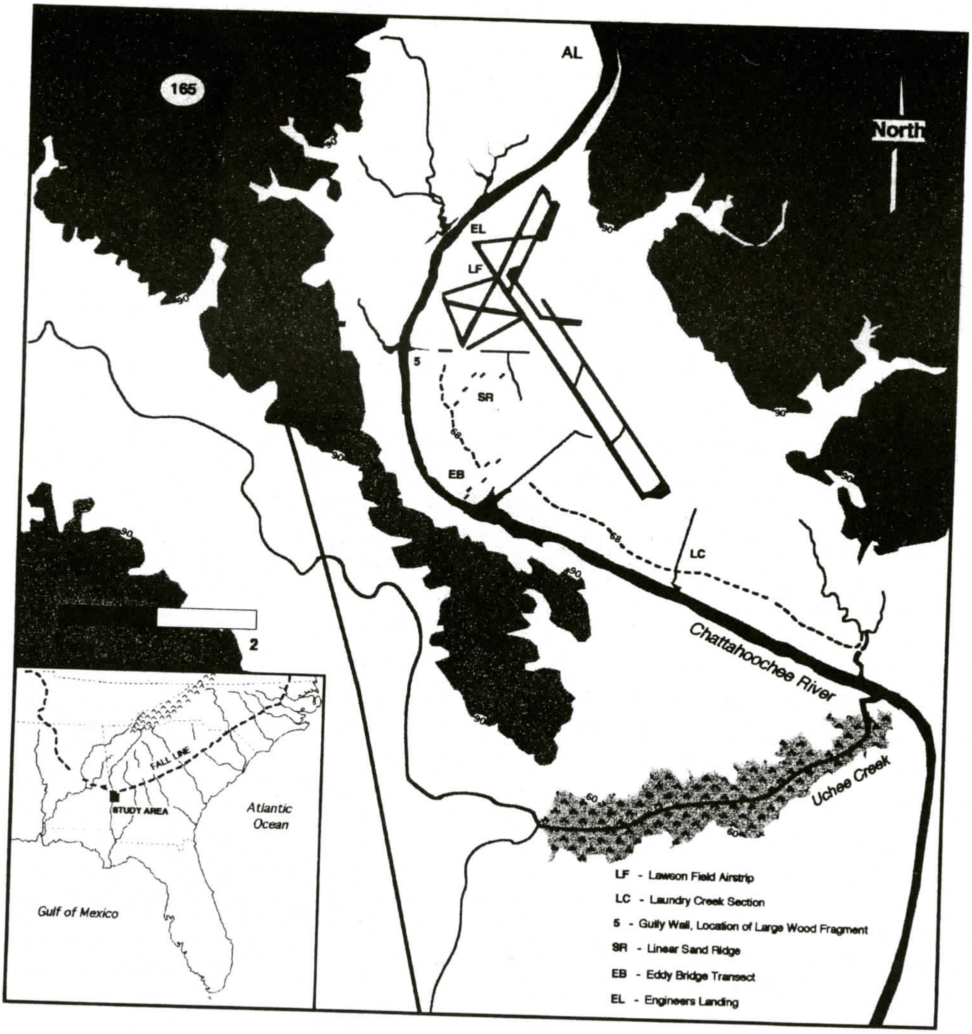

Figure 1. The Lawson Field study area in the lower Chattahoochee alluvial valley, Fort Benning, Georgia.

of the "Fall Line." Igneous and metamorphic basement rocks dip steeply basinward beneath Cretaceous sedimentary cover, and the Upper Cretaceous Eutaw and Blufftown formations (Eargle, 1955) account for approximately 50 m of claystone bedrock standing above mean sea level (asl) at Fort Benning. The present channel of the Chattahoochee River is characterized by wide meanders with a wavelength of over 5 km. The channel bottom in the thalweg was approximately 49 m asl prior to the construction of the Walter F. George dam (Toulmin and Lamoureaux, 1963, p. 390). This represents at least 10 m of incision below the much straighter paleovalley thalweg crossing Lawson Field.

Both the land surface morphology and the underlying stratigraphy in the Lawson Field study area suggest that the Chattahoochee River was actively downcutting and migrating to the west between 47 and 8 ka. The valley was filled episodically as the river downcut, resulting in a level terrace grade which extends upvalley and downvalley for most of the Americus 30'x60' quadrangle mapped by Reinhardt and others (1994). This surface is here named the Lawson Field Terrace and tentatively correlated with landforms elsewhere described as "Deweyville" terraces.

Table 1. New radiocarbon dates from Lawson Field, Fort Benning, Georgia.

Site	Elevation		Material	^{14}C yr B.P.	Lab Number
	m bls	m asl			
Location 5	5.0	59.0	Wood	46,950 ± 8,200	UGa-7250
Engineers Landing	2.3	62.0	Organic silt	7,300 ± 120	Beta-92643
Linear Sand Ridge, Tr 2	1.0	69.0	Organic silt	1,440 ± 90	Beta-92644
Eddy Bridge T-1, Tr 1	0.7	64.3	Charred wood	451 ± 45	UGa-7254
Location 9	0.5	65.0	Charred nutshell	242 ± 85	UGa-7253

The Lawson Field Terrace and Soil Stratigraphy on the Airstrip

A level terrace grade which averages 68 m asl was chosen as an appropriate location for the airstrip at Fort Benning in the 1930s (Cable and others, 1997, p. 95-102). This Lawson Field Terrace represents the second terrace (T-2) landform for these reaches of the Chattahoochee alluvial valley (see Figure 1). The river channel is incised more than 15 m below the terrace grade and confined to a narrow trench less than 150 m wide. There is consequently very little present "floodplain" although late Holocene overbank flood deposits are locally inset against the eroding T-2 scarp, forming a discontinuous first terrace (T-1) surface.

Up to a meter of landfill and concrete were added to construct the runways on the airstrip. This may have effectively sealed earlier plowzone and prehistoric midden deposits, and two small trenches excavated in the present investigations confirmed the potential for significant archaeological finds. In Trench 1, a relict plowzone (Ap horizon) was observed to truncate a cambic (Bw) horizon at approximately 45 centimeters below the land surface (cm bls). The Bw horizon contained prehistoric ceramics of the local Blackmon phase (A.D. 1625-1715).

In both trench profiles, a much older, strongly weathered subsoil (2Bt horizon) was encountered approximately 150 cm bls (66.5 m asl). Although truncated, the paleosol can be classified as an Ultisol (Soil Survey Staff, 1997, p. 55-56; Birkeland, 1984, p. 52) based on its approximately one meter thick kandic or argillic horizon (Figure 2). Thick, continuous clay films

Figure 2. Continuous clay film coating pedfaces, Trench 2, Lawson Field airstrip.

coat the surface of prismatic soil aggregates (peds) up to 5 cm long in cross-bedded sands which coarsen to contain quartzose pea gravels toward the base of the trench exposures, approximately 65 m asl.

Geotechnical borings performed for the army on the Lawson Field airstrip encountered at least 8 m of unconsolidated coarse sand and gravel without penetrating the underlying Cretaceous claystone bedrock. The entire package from the top of the truncated paleosol to the bedrock contact represents sediment deposited as the river downcut and migrated westward. Because the best exposure is found where this

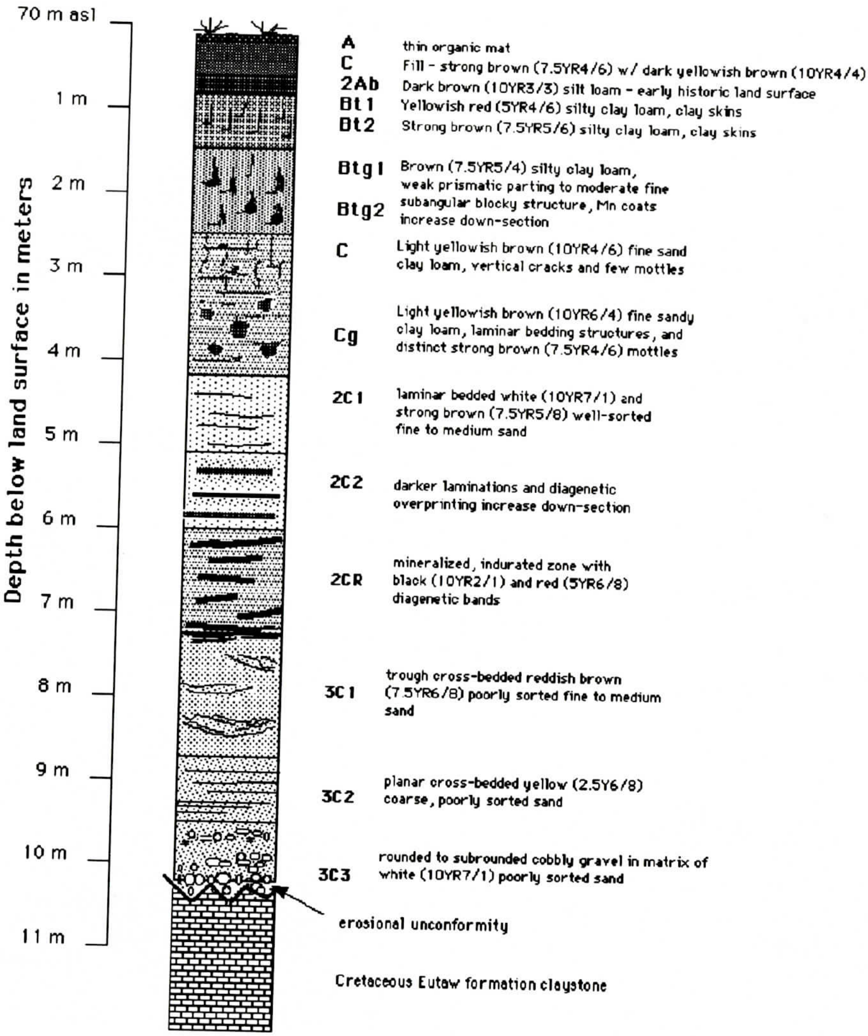

Figure 3. Stratigraphic column at Laundry Creek, Fort Benning, Georgia.

package has been cut by the southwest-trending channel of Laundry Creek, the principal formation which underlies the Lawson Field Terrace is here described from and named after that exposure.

The Laundry Creek Formation

The Laundry Creek Formation is a deposit of quartzose sand and gravel with planar and trough crossbeds up to a meter thick. These lithologic features alone make it traceable in outcrop and stratigraphic trenches from the type section across to the Alabama side of the Chattahoochee River and upstream above the prominent meander on Lawson Field. It is here being described for the first time as a formal lithostratigraphic unit.

The location of the type section is shown in Figure 1. The stratigraphic column is described in Figure 3 and the section is illustrated by Figures 4a-4c. The Laundry Creek Formation represents all but the upper 65 cm of the column above the bedrock contact at 60 m asl. Assuming an average 10 m thickness and a valley width of 3 km, the formation has a volume of 0.6 x $10^3 m^3$ if it is mappable for only 20 km up and down valley. On the quite reasonable as-

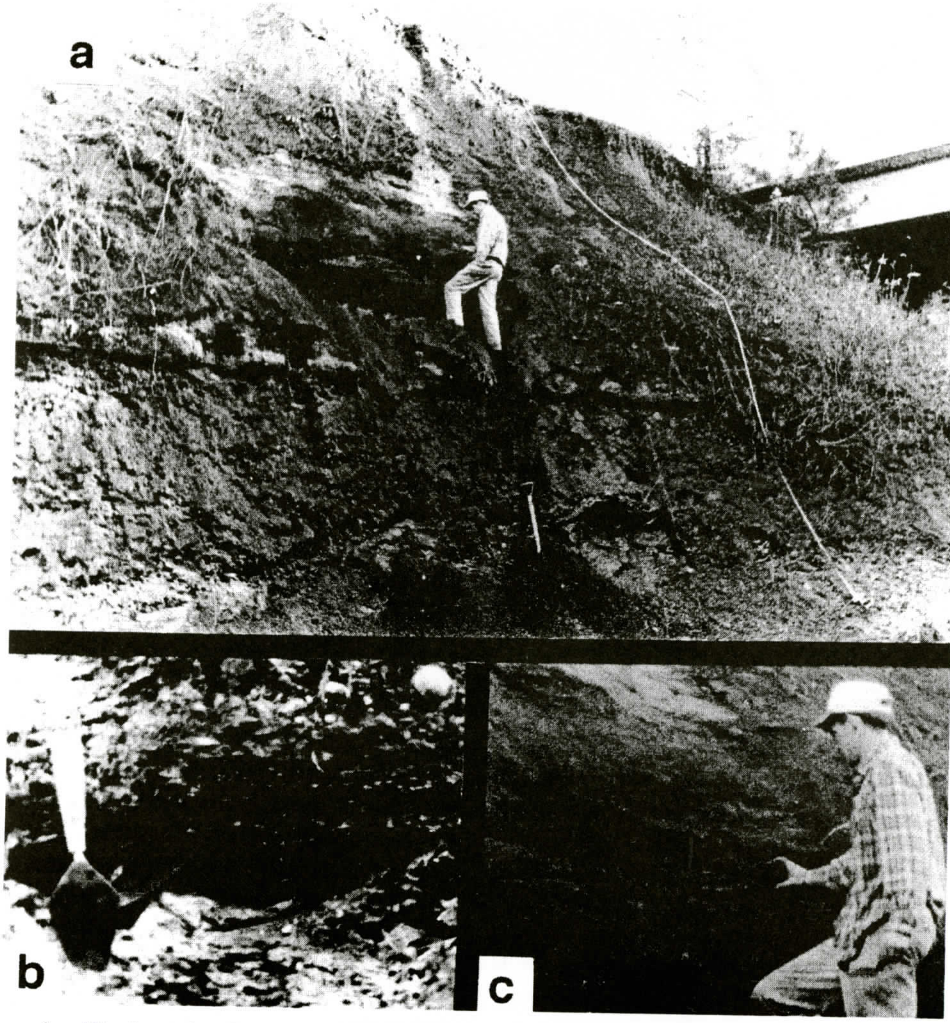

Figure 4. a. The Laundry Creek stratigraphic section. b. Unconformable contact between the Laundry Creek Formation and Cretaceous claystone. 4c. Planar and trough crossbed sedimentary structures in the Laundry Creek Formation.

sumption that it is mappable for 50 km the formation will have a volume of 2.5 x 10^3m^3, and if it were mappable all the way to the Florida state line it would have a volume of over 10 x 10^3m^3. Much of the Quaternary alluvium in the lower Chattahoochee valley is unfortunately submerged beneath the pools of Lake Walter F. George, Lake G. W. Andrews, and Lake Seminole although some reconstruction is possible using studies prior to dam construction (e.g. Roberts, 1958; Toulmin and LaMoreaux, 1963).

The base of the Laundry Creek section is an unconformable contact at which lateral migration of the ancestral Chattahoochee truncated the claystone bedrock (Figure 4b). Because this "bounding surface" can be expected to occur on progressively younger lithologies of Cretaceous, Tertiary, or even Quaternary age moving down valley, an allostratigraphic approach (NACOSN, 1983, p. 865-867) does not seem appropriate for describing the formation. Bedforms, clast size, sorting, and package thickness appear to be more reliable although bounding surfaces may prove traceable in future field studies. Soils or paleosols with thick kandic or argillic horizons do tend to occur at the upper

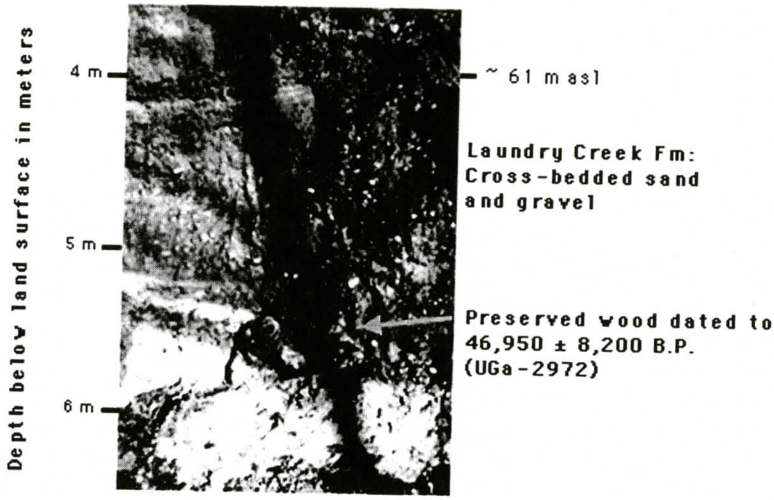

Figure 5. Radiocarbon-dated wood in situ below the Laundry Creek Formation at Location 5, Fort Benning, Georgia.

bounding surface, as typified by the Bt1, Bt2, Btg1, and Btg2 horizons of the type section.

In addition to relatively thick (meter scale) crossbeds, alternation of planar and trough bedforms characterize the Laundry Creek Formation (Figure 4c). This suggests abrupt changes in stream power and direction of flow which are typical of a braided stream (Miall, 1977; Williams and Rust, 1969; Shelton and Noble, 1974; Smith, 1971). Unfortunately, many bedforms at the type section have been overprinted by soil development and groundwater effects.

While no dateable organic specimens were collected from the type section, two radiocarbon dates obtained in the present investigations do bracket the age of the Laundry Creek Formation. A large fragment of wood was recovered from reduced clay above bedrock but underlying coarse cross-bedded sand and gravel, approximately 59 m asl, at Location 5 (Figure 5). An age of 46,950 ± 8,200 B.P. (UGa-7250) was obtained at the University of Georgia's Center for Applied Isotope Studies. This age is near the limit of conventional radiocarbon dating but such small activity above background can be measured by liquid scintillation (Long and Kalin, 1992a, 1992b; McCormac et al., 1993). It represents a maximum age, or terminus post quem, for the overlying Laundry Creek Formation.

A minimum age, or terminus ante quem, comes from fine textured alluvium inset against the eroded slipface of the Lawson Field Terrace at the Engineers Landing (EL on Figure 1). The organic residue from a silty sediment was dated to 7,360 ± 130 B.P. (Beta-92643). The sample was collected from approximately 62 m asl in an exposure two kilometers upstream and several hundred meters closer to the present channel thalweg than Location 5.

The upper boundary of the Laundry Creek Formation has been truncated by erosion along the scarp of the Lawson Field Terrace and by some aeolian reworking on the terrace surface itself. The lower boundary appears to dip down to the west but does not extend beneath the present river channel, which has been cut down into the underlying claystone bedrock. Isolated exposures of the Laundry Creek Formation were observed on the Alabama side of the Chattahoochee at approximately 60 m asl during the Lawson Field geomorphological investigations. Sand and gravel capping higher surfaces at over 90 m asl (Szabo and Copeland, 1988) are early Pleistocene or older and unrelated to the degradational sequence described in the present paper.

Linear Sand Ridge on the Lawson Field Terrace

A conspicuous sand ridge (SR on Figure 1) covers half of Lawson Field, rising 10 m above a swale to the southwest and 7 m above a swale to the northeast. Six trenches were excavated in a transect running across this ridge to determine its origin and potential for containing buried archaeological sites. Trench 1 was in the swale to the northeast and exposed coarse cross-bedded sediments of the Laundry Creek Formation. Silt drapes were noted in the laminar bedded sands at the west end of the trench and pebbly gravels were more abundant at the east end. The capping soil features a Bt horizon which is close to a meter thick.

Trench 2 was on the eastern slope of the ridge, exposing 80 cm of slump and aeolian mantle capping a weak paleosol formed in the Laundry Creek Formation. The organic residue from a sample collected at 80-100 cm bls in the paleosol was radiocarbon dated to 1,440 ± 90 B.P. (Beta-92644). This can be considered a minimum age for aeolian reworking of the Laundry Creek Formation, which has continued down to the present day.

Trench 3 was on top of the ridge and exposed unconsolidated, massively-bedded quartz sand. At Trench 4, sedimentary structures in the uppermost sandy sediments indicate aeolian additions along the ridge's western slope. The A-C trench profiles are consistent with mapped surface soils of the Entisol order. Slightly better developed soils of the Inceptisol order (A-Bw-C profiles) were observed on the western ridge slope at Trenches 5 and 6.

The linear sand ridge on Lawson Field is here interpreted as a primary fluvial deposit which is probably the uppermost bed of the Laundry Creek Formation. Dateable plant parts or organic residues within the loose, massively bedded sands are unlikely to return an age representative of the time of deposition. Prehistoric artifacts are common on the ridge surface, and it is possible that prehistoric cultural features intrude the loose sandy sediments or have been buried by slumping of the sort documented at Trench 2.

Terrace Complex at the Engineers Landing

The Engineers Landing (EL on Figure 1) is an artificially ramped surface cut from river grade at ca. 60 m asl up to the main road circling the airstrip, whose grade is ca. 65 m asl. Outcrops in the walls of a small gully were described and linked in a composite profile (Figure 6). The Laundry Creek Formation is represented by cross-bedded sand and gravel which dip riverward and pinch out approximately 50 m from the active river channel. Planar and trough crossbeds alternate cyclically upsection, indicating abrupt changes in stream power and direction of flow which are typical of a braided stream (Miall, 1977; Williams and Rust, 1969; Shelton and Noble, 1974; Smith, 1971).

Localized erosion is evident here and in other exposures where the land slopes up to the Lawson Field Terrace grade. Fine textured Holocene flood sediments have accreted against the eroded slipface of the coarser sand and gravel. Soils formed in these sediments lack the thick kandic or argillic horizons characteristic of those observed at Laundry Creek and on the airstrip. The profiles in Figure 6 would be classified as Inceptisols rather than Ultisols (Soil Survey Staff, 1997, p. 56-57; Birkeland, 1984, p. 47).

The organic residue from a bulk sample of fine sediment collected at 230 cm bls (ca. 61.7 m asl) was radiocarbon dated to 7,360 ± 130 B.P. (Beta-92643), confirming the Holocene age suspected from the relatively weak soil development. At this and other locations where space is afforded by the eroding banks of the river or its tributary gullies, Holocene overbank floods have built a discontinuous first terrace (T-1) whose grade is ca. 64 m asl. The radiocarbon date from the Engineer's Landing also provides a minimum age for the gravelly channel sands at 61-63 m asl against which the finer textured sediment is embanked.

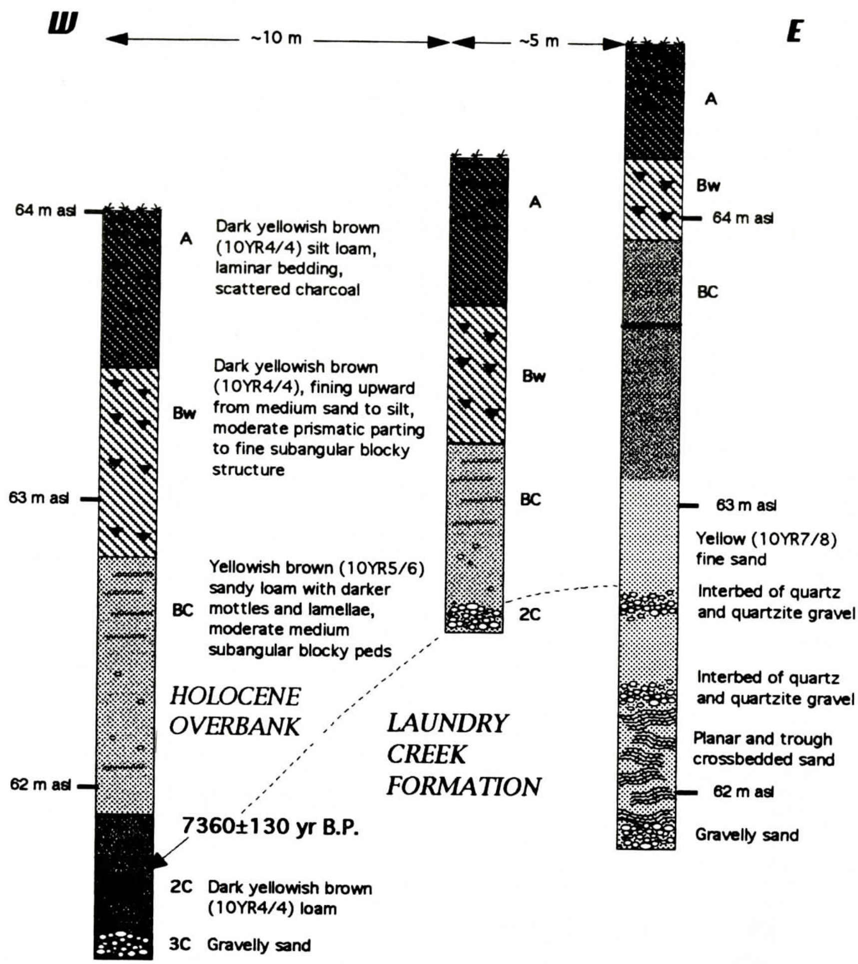

Figure 6. Composite profile for exposure at Engineers Landing, Fort Benning, Georgia.

Lawson Field Terrace Scarp and Inset Alluvium Downstream of Eddy Bridge

The grade of the Lawson Field Terrace (T-2) rises gradually downstream of the airstrip so that it averages 69 m asl at Eddy Bridge and 70 m asl at Laundry Creek. A long backhoe trench downstream of Eddy Bridge on the pronounced T-2 scarp allowed examination of the underlying alluvial stratigraphy. The disrupted stratigraphy illustrated by Figure 7 suggests the possible influence of late Pleistocene tectonic uplift (e.g. Carver and Waters, 1984; Reinhardt and others, 1984; Winker and Howard, 1977). Alternatively, this disturbance may be the result of localized slumping following river bank undercutting. The soil profiles examined in two trenches on the Lawson Field Terrace (T-2) surface itself showed increasingly developed clay films and deeper hues in the subsoil horizons compared to profiles on the adjoining T-1.

The T-1 is much wider at Eddy Bridge than at the Engineers Landing and eventually flanks the extensive modern floodplain at the mouth of Uchee Creek. A soil with a relatively thin (ca. 50 cm) kandic or argillic horizon has formed across the top of sediments representing several microenvironments of the earlier Holocene floodplain. While slackwater silts and clays were at the base of the Trench 1 section, coarser sands at the base of Trench 2 clearly represent a "natural levee" microenvironment (Leopold

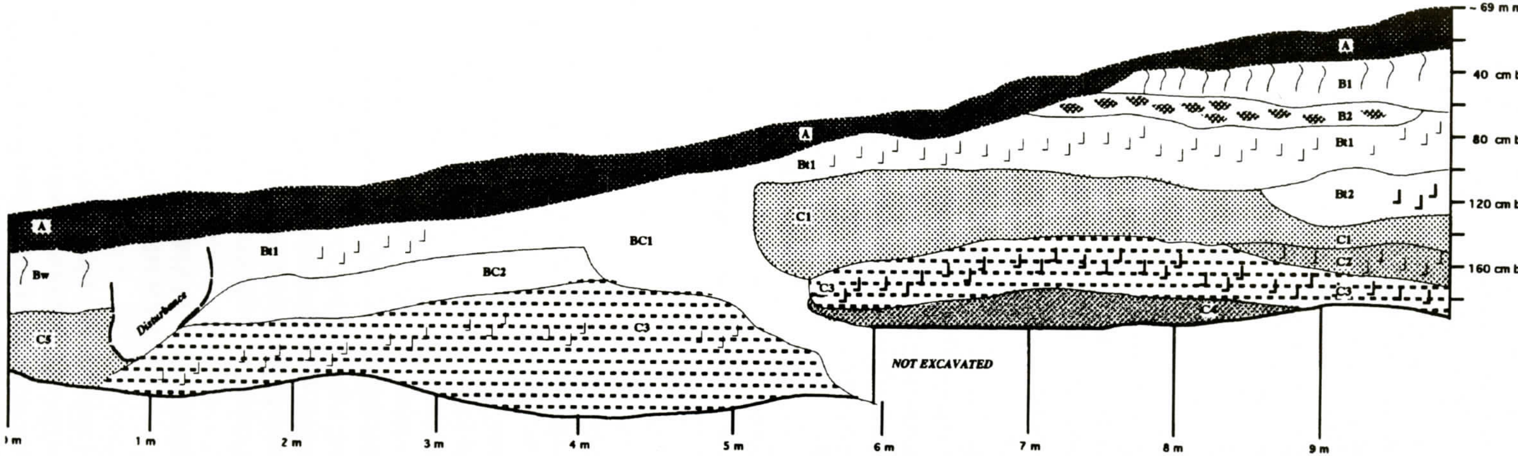

A - Brown (7.5YR4/3-4/4) sandy loam, loose, massive, many fine to medium roots

Bw - Strong brown (7.5YR4/6-5/6) sandy loam, moderate medium subangular blocky structure, few medium-sized roots

Bt1 - Strong brown (7.5YR5/6) sandy clay loam, moderate medium subangular blocky structure, thin but continuous clay films on ped faces, intensely rooted at the top

BC1 - Mixed, (tectonically?) disturbed deposit of brownish yellow (10YR6/6-6/8) medium sand with intrusive chunks of strong brown (7.5YR4/6-5/6) sandy clay loam

BC2 - Brownish yellow (10YR6/6-6/8) medium sand withstrong brown (7.5YR4/6-5/6) mottles; thin, discontinuous clay films

C5 - Yellowish brown to brownish yellow (10YR5/6-6/6) fine to medium sand; compact, massively bedded

B1 - Yellowish brown (10YR5/4) sandy loam with strong brown (7.5YR5/6) mottling, very weak fine subangular blocky structure; much intrusive fill indicated by soda bottles, cans, other modern refuse;charcoal lenses

B2 - Strong brown (7.5YR4/6-5/6) sandy loam, weak medium subangular blocky structure, few medium-sized roots

Bt2 - Yellowish brown (10YR5/4-56) sandy clay loam, strong medium subangular blocky structure, thick continuous clay films on ped faces

C1 - Brownish yellow (10YR6/6-6/8) fine to medium sand; loose, massively bedded; more compact with some weak medium subangular blocky structure at the top

C2 - Brownish yellow (10YR6/6-6/8) fine to medium sand; compact, massively bedded; weak medium subangular blocky structure

C3 - Strong browni(7.5YR5/6-6/8) sandy clay loam; compact, massively bedded; moderate medium subangular blocky structure

C4 - Yellowish brown (10YR5/6) sandy loam; loose, massively bedded

Figure 7. Profile looking NW of Trench 3 downstream of Eddy Bridge, Fort Benning, Georgia.

and others, 1964, p. 317). Scattered charcoal fragments collected from 50-70 cm bls in Trench 1 were radiocarbon dated by the University of Arizona accelerator facility to 451 ± 45 B.P. (UGa-7254). This suggests one or more natural or cultural burning episodes in protohistoric times in this part of the alluvial valley.

REGIONAL CORRELATES FOR THE LAUNDRY CREEK FORMATION

The above geomorphological and stratigraphic reconstructions for the Lawson Field study area suggest that the Chattahoochee River was actively downcutting and migrating to the west between 47 and 8 ka. Similar degradational sequences are found in most alluvial valleys in the Southeast during the late Pleistocene and early Holocene, particularly at and immediately downstream of the Fall Line.

Surfaces constructed during valley degradation in Alabama (Maxwell, 1971; Szabo, 1973), the Mississippi alluvial valley (Saucier, 1994, p. 240-242; Autin et al., 1991), and Texas (Blum et al., 1995a, 1995b) are traditionally referred to as "Deweyville" terraces. Deweyville terraces are typically found flanking underfit trunk streams which were laterally migrating and actively downcutting during the late Pleistocene. Large arcuate paleomeanders are also characteristic although not a defining or lithostratigraphic feature. While there do not appear to be paleomeanders on the Lawson Field Terrace in the reaches studied, some are apparent downstream of the confluence with Uchee Creek and along Uchee Creek itself.

In the Atlantic Coastal Plain, a similar degradational sequence was constructed as the Savannah River migrated to the Georgia side downstream of the Fall Line at Augusta (Nystrom and Denham, 1999; Leeth and Nagle, 1996). The lithostratigraphic unit mapped as Qal2 by Leeth and Nagle appears to be late Pleistocene. Qal2 was formed by a cyclic pattern of entrenchment and subsequent infilling, which gave rise to an irregular basal contact. Afterwards, the river migrated to the southwest and began a period of downcutting that continued until it reached a maximum incision of 15 m into the underlying Tertiary cover.

The Piedmont reaches of the Savannah River were studied by Segovia (1985) and Schuldenrein (1996, p. 11-17) prior to impoundment by the Richard B. Russell reservoir. Segovia inferred a braided stream system responsible for deposition of his Pleistocene McCalla Formation, which appears to be a Piedmont equivalent of the Qal2 of Leeth and Nagle (1996). At 50 ka the river was on the South Carolina side of McCalla Island, and it shifted laterally to the Georgia side by the early Holocene. The McCalla Formation was present in the sterile, basal levels of the Gregg Shoals archaeological site, and the overlying, artifact-rich alluvium was designated the Gregg Shoals Formation (Segovia, 1985).

Studies along the Ogeechee River by Leigh and Feeney (1995) are particularly significant since this stream flows on the Coastal Plain for almost its entire length and it has yet to be dammed or channelized by man. Radiocarbon dates on organic material immediately above channel sands suggest that large arcuate paleomeanders were active at approximately 31-28 and 8.5-4.5 ka. Because the channel-bed elevation was essentially the same as, or slightly higher than, that of the modern channel bed, Leigh and Feeney infer that there was no lowering of base level in response to eustatically lower sea levels during the Pleistocene.

Terrace of the Oconee River were mapped by Brook (1981) from Athens downstream to the dam for the Wallace Reservoir. Brook's Barnett Shoals Terrace appears to be equivalent in age and mode of deposition to the Lawson Field Terrace as defined above. Cosner (1973) investigated the stratigraphy of the Ocmulgee River alluvial valley and described over 3 m of Holocene deposits inset against the older Macon Plateau alluvial terrace.

POSSIBLE CAUSES OF REGION-WIDE VALLEY DEGRADATION

Data from this and other studies indicate that the degradational sequence in the Chattahoochee alluvial valley is part of a regional pattern. Several mechanisms could cause regional degradation of alluvial valleys ca. 47-8 ka. One would be lowered base level at the last glacial maximum (Fisk, 1944). The fact that incision into bedrock has continued during the Holocene, when sea level is rising, suggests that other mechanisms must be involved. Recent studies by Saucier (1994, 1981), Blum and Valastro (1994), and Leigh and Feeney (1995) also question the upstream effects of lowered sea level on Coastal Plain river valleys.

Climatic explanations offered to date reflect uncertainty about late Pleistocene conditions in the Southeast. Cool, moist conditions of waxing glaciation are proposed for Deweyville deposition by Saucier (1981, p. 12) while Leigh and Feeney (1995) propose intensified summer monsoon conditions for increased discharge in the Ogeechee River.

Future studies may reconcile these apparently conflicting reconstructions by attention to millenial-scale variation. In the 200 thousand year chronology of river response to climate recently developed for southern Europe (Fuller et al., 1998), for example, episodes of incision occurred during warmer interstadial and interglacial periods. Fourteen such intervals are now recorded between the present interglacial and Heinrich event H5, ca. 50 ka.

While additional age constraints from radiocarbon dating may be possible, coarse sand and gravel deposits such as the Laundry Creek Formation unfortunately tend to lack dateable organic materials. New methods of dating such as optically stimulated luminescence (OSL) may be better suited to the task of identifying intervals of deposition on a millenial time scale (Ivester and Godfrey-Smith, 1999; Ivester and others, 1999).

The coincidence of the accentuated scarp of the Lawson Field Terrace and apparent disruption of subsurface stratigraphic contacts observed in the present study argues for some tectonic dimension to the evolution of valley landforms. Perhaps the cause is still ultimately glacioeustatic (cf. Walcott, 1972), although channel migration to the west is common to a number of Coastal Plain valleys. The present and previous studies (Carver and Waters, 1984; Reinhardt and others, 1984; Winker and Howard, 1977) clearly suggest the need for systematic paleoseismic or "archaeo" seismic (Tuttle and Schweig, 1995; Noller and Lightfoot, 1997) field investigations. Such investigations can constrain the scale and magnitude of regional uplift and movement along specific faults.

REFERENCES CITED

Autin, W. J., Burns, S. F., Miller, B. J., Saucier, R. T., and Snead, J. I., 1991, Quaternary geology of the lower Mississippi Valley, in Morrison, R. B., ed., Quaternary Nonglacial Geology: Conterminous U.S., p. 547-582: Geological Society of America, Boulder, Colorado.

Birkeland, P. W., 1984, Soils and Geomorphology: Oxford University Press, New York.

Blum, M. D., and Valastro, S. Jr., 1993, Late Quaternary sedimentation, Lower Colorado River, Gulf Coastal Plain of Texas: Geological Society of America Bulletin, v. 106, p. 1002-1016.

Blum, M. D., Morton, R. A., and Durbin, J. M., 1995a, "Deweyville" terraces and deposits of the Texas Gulf Coastal Plain: Transactions of the Gulf Coast Association of Geological Societies, v. 45, p. 53-60.

Blum, M. D., Morton, R. A., and Durbin, J. M., 1995b, "Deweyville" terraces and deposits of the Texas Gulf Coastal Plain: a reevaluation: American Association of Petroleum Geologists Bulletin, v. 79, no. 10, p. 1554.

Brook, George A., 1981, Geoarcheology of the Oconee reservoir: Wallace Reservoir Project Contribution No. 15, Department of Anthropology, University of Georgia, Athens.

Cable, J. S.,O'Steen, L. D., Reed, M. B., and Joseph, J. W., 1997, Cultural Resources Survey, Lawson Army Airfield, Ft. Benning, Georgia and Alabama: New South Associates Report No. 447, Atlanta, Georgia.

Carver, R. E., and Waters, S. A., 1984, Fluvial terraces and late Pleistocene tectonism in Georgia: Southeastern Geology, v. 25, no. 2, p. 117-122.

Cosner, O. J., 1973, Stratigraphy of an Archaeological Site, Ocmulgee Flood Plain, Macon, Georgia: U. S. Geological Survey Water Resources Investigations 54-73, Atlanta, Georgia.

Eargle, D. H., 1955, Stratigraphy of the outcropping Cretaceous rocks of Georgia: U. S. Geological Survey Bulletin 1014, Washington, D. C.

Fisk, H. N., 1944, Geological investigation of the alluvial valley of the lower Mississippi River: U. S. Army Corps of Engineers, Mississippi River Commission, Vicksburg, Mississippi.

Fuller, I. C., Macklin, M. G., Lewin, J., Passmore, D. G., and Wintle, A. G., 1998, River response to high-frequency climate oscillations in southern Europe over the past 200 k.y.: Geology, v. 26, no. 3, p. 275-278.

Ivester, A. H., and Godfrey-Smith, D. I., 1999, Optically stimulated luminescence properties of eolian sediments in the Georgia Coastal Plain: Georgia Journal of Science. v. 57, no. 1, p. 56-57.

Ivester, A. H., Leigh, D. S., and Godfrey-Smith, D. I., 1999, Paleoenvironmental implications of Georgia's source bordering riverine dunes: GSA Abstracts, v. 31, no. 3, p. A-23.

Leeth, D. C., and Nagle, D. D., 1996, Shallow subsurface geology of part of the Savannah River alluvial valley in the upper Coastal Plain of Georgia and South Carolina: Southeastern Geology, v. 36, no. 1, p. 1-14.

Leigh, David S., and Feeney, Thomas P., 1995, Paleochannels indicating wet climate and lack of response to lower sea level, southeast Georgia: Geology, v. 23, p. 687-690.

Leopold, L. B., Wolman, M. G., and Miller, J. P., 1964, Fluvial processes in geomorphology: W. H. Freeman, San Francisco.

Long, A., and Kalin, R. M., 1992a, Use of Liquid Scintillation Counting for Radiocarbon Dating in the 50,000 to 65,000 yr Range: Determination of Chemical Blank and Fossil Wood: Radiocarbon, v. 34, no. 3, p. 351-359.

Long, A., and Kalin, R. M., 1992b, Radiocarbon Dating of Samples in the 50,000 to 65,000 ybp Range without Isotopic Enrichment, in Povinec, P., editor, Rare Nuclear Processes, p. 256-263.

McCormack, F. G., Kalin, R. M., and Long, A., 1993, Radiocarbon Dating Beyond 50,000 Years by Liquid Scintillation Counting, in Noakes, J. E., Schonhofer, F., and Polachs, H. A., editors, Liquid Scintillation Spectrometry, p. 125-133.

Maxwell, R. W., 1971, Origin and Chronology of Alabama River Terraces: Transactions of the Gulf Coast Association of Geological Societies, v. 21, p. 83-95.

Miall, A. D., 1977, A Review of the Braided-river Depositional Environment: Earth-Science Reviews, v. 13, p. 1-62.

Noller, J. S., and Lightfoot, K. G., 1997, An Archaeoseismic Approach and Method for the Study of Active Strike-Slip Faults: Geoarchaeology, v. 12, no. 2, p. 117-135.

North American Commission on Stratigraphic Nomenclature (NACOSN), 1983, North American stratigraphic code: American Association of Petroleum Geologists, v. 67, p. 841-875.

Nystrom, P. G., Jr., and Denham, M. F., 1999, Fluvial terraces in the Upper Coastal Plain section of the Savannah River valley: GSA Abstracts, v. 31, no. 3, p. A-57.

Reinhardt, J. R., Prowell, D. C., and Christopher, R. A., 1984, Evidence for Cenozoic tectonism in the southwest Georgia Piedmont: Geological Society of America Bulletin, v. 95, p. 1176-1187.

Reinhard, J., Schindler, J. S., and Gibson, T. G., 1994, Geologic map of the Americus 30'x60' quadrangle, Georgia and Alabama, U. S. Geological Survey Map I-2174.

Roberts, W. B., 1958, A Study of River Terraces of the Chattahoochee River between Chattahoochee, Florida, and Fort Gaines, Georgia: M. S. thesis, Florida State University, Tallahassee.

Saucier, R. T., 1981, Current thinking on riverine processes and geologic history as related to human settlement in the southeast: Geoscience and Man, v. 22, p. 7-18.

Saucier, R. T., 1994, Geomorphology and Quaternary Geologic History of the Lower Mississippi Valley: Mississippi River Commission, Vicksburg, Mississippi.

Schuldenrein, J., 1996, Geoarchaeology and the mid-Holocene landscape history of the Greater Southeast, in Anderson, D. G., editor, The Mid-Holocene in the Southeast, p. 3-27.:University of Florida Press, Gainesville, Florida.

Segovia, A. V., 1985, Archeological Geology of the Savannah River Valley and Main Tributaries in the Richard B. Russell Multiple Resource Area: National Park Service, Atlanta, Georgia.

Shelton, J. W., and Noble, R. I., 1974, Depositional features of braided and meandering streams: American Association of Petroleum Geologists Bulletin, v. 58, p. 742-759.

Smith, N. D., 1971, Transverse bars and braiding in the lower Platte River, Nebraska: Geological Society of America Bulletin, v. 87, p. 3407-3420.

Soil Survey Staff, 1997, Keys to Soil Taxonomy: Pocahontas Press, Blacksburg, Virginia.

Szabo, M. W., 1973, Deweyville Terrace, Alabama River basin, Alabama: The Journal of the Alabama Academy of Science, v. 44, no. 3, p. 189.

Szabo, M. W., and Copeland, C. W., Jr., 1988, Geologic Map of Alabama: Geological Survey of Alabama Special Map 220, Montgomery, Alabama.

Toulmin, L. D., and LaMoreaux, P. E., 1963, Stratigraphy along Chattahoochee River, connecting link between the Atlantic and Gulf Coastal Plains: American Association of Petroleum Geologists Bulletin, v. 47, p. 849-884.

Tuttle, M. P., and Schweig, E. S., 1995, Archaeological and Pedological Evidence for Large Prehistoric Earthquakes in the New Madrid Seismic Zone, Central United States: Geology, v. 23, p. 253-256.

Walcott, R. I., 1972, Late Quaternary vertical movements in eastern North America: quantitative evidence of glacio-isostatic rebound: Review of Geophysics and Space Physics, v. 10, p. 849-884.

Williams, P. F., and Rust, B. R., 1969, The sedimentology of a braided river: Journal of Sedimentary Petrology, v. 39, p. 649-679.

Winker, C. D., and Howard, J. D., 1977, Correlation of tectonically deformed shorelines on the southern Atlantic coastal plain: Geology, v. 5, p. 123-127.